HUMAN GENE THERAPY 21:65–74 (January 2010)

DOI: 10.1089/hum.2009.106

Enhanced Transfection Efficiency into Macrophages and Dendritic Cells by a Combination Method Using Mannosylated Lipoplexes and Bubble Liposomes with Ultrasound Exposure

Keita Un,[1] Shigeru Kawakami,[1] Ryo Suzuki,[2] Kazuo Maruyama,[2] Fumiyoshi Yamashita,[1] and Mitsuru Hashida[1,3]

Abstract

To achieve effective gene therapy, it is necessary to selectively and efficiently transfect therapeutic gene into targeted cells. In this study, we developed a combination method using mannosylated lipoplexes, which show selectivity to antigen-presenting cells such as macrophages and dendritic cells, and bubble liposomes (BLs), which are known to enhance transfection efficiency on exposure to ultrasound (US). In cultured mouse macrophages, known for the expression of mannose receptors, the transfection efficiency of this combination method using mannosylated lipoplexes and BLs with US was higher than that of naked pDNA or unmodified lipoplexes and BLs. In the liver and spleen, the *in vivo* transfection efficiency of this combination method was significantly higher than that of naked pDNA or unmodified lipoplexes and BLs with US. Transfection in hepatic nonparenchymal cells using this combination method was about 12 times higher than that in hepatic parenchymal cells. As far as splenic transfection activities were concerned, the transfection efficiency of this combination method in $CD11c^+$ cells was significantly higher than that in $CD11c^-$ cells. In conclusion, we demonstrated that the gene transfection efficiency in macrophages and dendritic cells was significantly increased by this combination method using mannosylated lipoplexes and BLs with US exposure.

Introduction

GENE THERAPY has been shown to be a promising medical treatment for specific diseases that involve gene mutations, such as cystic fibrosis and cancer. However, there are a number of barriers that hinder the achievement of effective gene therapeutic effects (Niidome and Huang, 2002). In addition, as it is essential to transfect gene into targeted cells to achieve effective gene therapy, novel gene transfection methods that can be used for transfection of targeted cells selectively and efficiently are necessary.

The antigen-presenting cells (APCs), which are the major target cells for cancer immunotherapy or antiinflammatory therapy, express large number of mannose receptors on the cell membrane (Taylor *et al.*, 2005). We have developed mannosylated liposomes for delivery to the APCs by mannose receptor-mediated endocytosis (Kawakami *et al.*, 2000; Yamada *et al.*, 2004; Wijagkanalan *et al.*, 2008). Recently, we have demonstrated that mannosylated liposomes targeted to APCs, such as macrophages and dendritic cells, can be applied to treatment of inflammatory diseases or cancer (Hattori *et al.*, 2006a,b; Higuchi *et al.*, 2006; Huang *et al.*, 2009). However, for achievement of better therapeutic effects which can be applied to actual medical treatment, higher transfection efficiency in APCs is necessary.

Recently, the uses of external physical stimulation, such as electrical, magnetic field, and water pressure, have been reported to improve gene transfection (Scherer *et al.*, 2002; Gersting *et al.*, 2004; Kobayashi *et al.*, 2004; Kim *et al.*, 2008). Among them, ultrasound (US) exposure method using microbubbles, used as contrast agents for US imaging, is one of the most promising approaches for enhanced gene transfection (Iwanaga *et al.*, 2007; Negishi *et al.*, 2008; Shen *et al.*, 2008; Suzuki *et al.*, 2008). It was reported that direct injection of naked pDNA and bubble liposomes (BLs) following US exposure showed high gene transfection efficiency (Negishi

[1]Department of Drug Delivery Research, Graduate School of Pharmaceutical Sciences, Kyoto University, Kyoto 606-8501, Japan.
[2]Department of Biopharmaceutics, School of Pharmaceutical Sciences, Teikyo University, Kanagawa 229-0195, Japan.
[3]Institute for Integrated Cell-Material Sciences, Kyoto University, Kyoto 606-8302, Japan.

et al., 2008; Suzuki *et al.*, 2008). However, the effectiveness of direct injection of naked pDNA is limited in the injection site. Therefore, systemic administration is necessary to transfect the gene widely in the organ. In addition, the delivery of pDNA to the targeted cells is also necessary to transfect the gene into them. As our mannosylated lipoplex can deliver pDNA efficiently into mannose receptor-expressing cells via intravenous route (Kawakami *et al.*, 2000; Yamada *et al.*, 2004), we considered that the combination of mannosylated lipoplexes and BLs is expected to enhance the transfection efficiency in those cells.

In this study, we developed the combination method using mannosylated lipoplexes and BLs with US to enhance gene transfection in mannose receptor-expressing cells. We investigated gene expression and cellular toxic properties in *in vitro* and *in vivo* by the combination method using mannosylated lipoplexes and BLs with US. In addition, the gene expression characteristics in nonparenchymal cells (NPCs) in the liver and dendritic cells in the spleen were also evaluated. The luciferase gene (pCMV-Luc) was used as reporter gene because it is simple to handle and can be detected with high sensitivity.

Materials and Methods

Materials

Dioleoylphosphatidylethanolamine (DOPE) was purchased from Avanti Polar Lipids (Alabaster, AL). 1,2-Distearoyl-sn-glycero-3-phosphocholine (DSPC) and collagenase type I were obtained from Sigma Chemicals (St. Louis, MO). Anti-CD11c monoclonal antibody (N418)-labeled magnetic beads were purchased from Miltenyi Biotec (Auburn, CA). 1,2-distearoyl-*sn*-glycero-3-phosphoethanolamine-*N*-[methoxy (polyethylene glycol)-2000] (DSPE-PEG(2K)) was obtained from NOF (Tokyo, Japan) and fetal bovine serum (FBS) was purchased from Equitech-Bio (Kerrville, TX). RPMI-1640, thioglycolate medium, and Hank's medium were purchased from Nissui Pharmaceutical (Tokyo, Japan). Opti-MEM I was obtained from Gibco BRL (Grand Island, NY). All other chemicals were of the highest purity available.

Mice

Female ICR mice (4–5 weeks, 18–22 g) were purchased from the Shizuoka Agricultural Cooperative Association for Laboratory Animals (Shizuoka, Japan). All animal experiments were carried out in accordance with the Principles of Laboratory Animal Care as adopted and propagated by the U.S. National Institutes of Health and the Guidelines for Animal Experiments of Kyoto University.

Construction and preparation of pDNA (pCMV-Luc)

pCMV-Luc was constructed by subcloning the HindIII/Xba I firefly luciferase cDNA fragment from pGL3-control vector (Promega, Madison, WI) into the polylinker of pcDNA3 vector (Invitrogen, Carlsbad, CA). pDNA was amplified in the *Escherichia coli* strain DH5α and was isolated and purified using a JETSTAR2.0 Plasmid Giga Kit (Genomed, Lohne, Germany).

Construction of lipoplexes and BLs

Man-C4-Chol or DC-Chol and DOPE were mixed in chloroform at a molar ratio of 3:2 to produce lipoplexes. Man-C4-Chol was synthesized by the method described previously (Kawakami *et al.*, 2000). For construction of BLs, DSPC and DSPE-PEG(2K) were mixed in chloroform at a molar ratio of 94:6. The mixture for the construction of each type of liposome was dried by evaporation, and then it was vacuum-desiccated and the resultant lipid film was resuspended in sterile 5% dextrose or saline. After hydration for 30 min at room temperature, the dispersion was sonicated for 10 min in a bath sonicator and for 3 min in a tip sonicator to produce liposomes. The resultant liposomes were sterilized by passage through a 0.45-μm filter (Nihon-Millipore, Tokyo, Japan). The particle sizes and zeta potentials of liposomes were determined using a Zetasizer Nano ZS instrument (Malvern Instruments, Worcestershire, UK). Lipoplexes were prepared at a charge ratio of 1.0:3.1 (−:+) as described in our previous report (Hattori *et al.*, 2004). BLs were prepared according to a previous report (Suzuki *et al.*, 2008). Briefly, 2 ml of liposomes was added to 5-ml sterilized vials, filled with perfluoropropane gas (Takachiho Chemical Ind., Tokyo, Japan), capped, and then pressured with 7.5 ml of perfluoropropane gas. To produce BLs, the vial was sonicated using a bath-type sonicator (As One Corporation, Osaka, Japan) for 5 min.

Harvesting and culture of macrophages

Mouse peritoneal macrophages were collected and cultured according to the previous report of our group (Hattori *et al.*, 2006b). Briefly, macrophages were harvested from ICR mice for 4 days after intraperitoneal injection of 2.9% thioglycolate medium. The washed cells were suspended in RPMI-1640 medium supplemented with 10% heat-inactivated FBS, penicillin G (100 U/ml), and streptomycin (100 μg/ml). Then, macrophages were plated on 24-well culture plates at a density of 2×10^5 cells/1.88 cm^2. After incubation for 2 hr at 37°C in 5% CO_2–95% air, nonadherent cells were washed off with culture medium and cells were incubated for another 72 hr.

In vitro *transfection experiments in macrophages*

After 72 hr incubation of macrophages, the culture medium was replaced with Opti-MEM-I-containing lipoplexes (5 μg pCMV-Luc/well). After 30 min incubation, BLs (60 μg/well) were added and macrophages were immediately exposed to US (frequency, 2.062 MHz; duty, 50%; burst rate, 10 Hz; intensity, 4.0 W/cm^2) for 20 sec using a 6-mm-diameter probe placed in the well. US was generated using a Sonopore-4000 sonicator (Nepa Gene, Chiba, Japan). Thirty minutes later, the incubation medium was replaced with RPMI-1640 again and incubated for an additional 23 hr. Lipofectamine® 2000 (LF2000; Invitrogen) was used according to the recommended procedures and the exposure time of LF2000 was the same as that for the mannosylated lipoplexes in *in vitro*. The cells were scraped from the plates and suspended in lysis buffer (0.05% Triton X-100, 2 m*M* ethylenediaminetetraacetic acid (EDTA), 0.1 *M* Tris, pH 7.8). Then, the cell suspension was shaken and centrifuged at 10,000×*g*, 4°C for 10 min. The supernatant was mixed with luciferase assay buffer (Picagene; Toyo Ink, Tokyo, Japan) and luciferase activity was measured in a luminometer (Lumat LB 9507; EG&G Berthold, Bad Wildbad, Germany). The luciferase activity was normalized with respect to the protein content of cells. The protein concentration

was determined with a Protein Quantification Kit (Dojindo Molecular Technologies, Tokyo, Japan).

In vitro *imaging of pDNA and lipoplexes in macrophages*

At 72 hr incubation after collecting macrophages, the culture medium was replaced with Opti-MEM-I-containing nitrobenzoxadiazole (NBD)-labeled liposomes/rhodamine-labeled pDNA complexes (1 μg pCMV-Luc/well). Rhodamine-labeled pDNA was prepared using the Label IT Nucleic Acid Labeling Kit (Mirus, Madison, WI). NBD-labeled liposomes consisted of Man-C4-Chol, DOPE, and NBD-DOPE in a molar ratio of 60:35:5. After preparation of NBD-labeled liposomes, free NBD-DOPE was removed by gel chromatography using a Sephadex® G-25 M PD-10 column (GE Healthcare, Uppsala, Sweden). Thirty minutes later, BLs (60 μg/well) were added and macrophages were exposed to US. After 30 min incubation, the incubation medium was replaced with RPMI-1640 and macrophages were incubated for an additional 5 hr and examined by fluorescence microscopy (Biozero BZ-8000; Keyence, Osaka, Japan).

In vivo *gene expression experiments in mice*

Four-week-old ICR female mice were given an intravenous injection of 300 μl lipoplexes via tail vein, using a 26-gauge syringe needle at a dose of 50 μg pDNA. Then, at 5 min after injection, BLs (500 μg/200 μl) were administered intravenously via tail vein. At 5 min after the injection of BLs, US (frequency, 1.045 MHz; duty, 50%; burst rate, 10 Hz; intensity, 1.0 W/cm^2; time, 2 min) was applied transdermally to the abdominal area using a Sonopore-4000 sonicator with a probe of diameter 20 mm. The organs were directly exposed to US, using a probe of diameter 6 mm. At predetermined times after injection, mice were sacrificed and their organs collected for each experiment. The organs were washed twice with cold saline and homogenized with lysis buffer (0.05% Triton X-100, 2 m*M* EDTA, 0.1 *M* Tris, pH 7.8). The lysis buffer was added at a weight ratio of 5 ml/g for liver or 4 ml/g for other organs. After three cycles of freezing and thawing, the homogenates were centrifuged at 10,000×*g*, 4°C for 10 min and the resultant supernatant was used for luciferase assay.

Cellular localization of luciferase activity in liver

At 6 hr after transfection, each mouse was anesthetized with pentobarbital sodium (40–60 mg/kg) and the liver was perfused with perfusion buffer (Ca^{2+}, Mg^{2+}-free HEPES solution, pH 7.2) for 10 min. Then, the liver was perfused with collagenase buffer (HEPES solution, pH 7.5, containing 5 m*M* $CaCl_2$ and 0.05% (w/v) collagenase type I) for 5 min. Immediately after the start of perfusion, the vena cava and aorta were cut and the perfusion rate was maintained at 5 ml/min. At the end of perfusion, the liver was excised. The cells were dispersed in ice-cold Hank's HEPES buffer by gentle stirring and then filtered through cotton mesh sieves, followed by centrifugation at 50×*g* for 1 min. The pellets containing parenchymal cells (PCs) were washed five times with Hank's HEPES buffer by centrifuging at 50×*g* for 1 min. The supernatant containing NPCs was similarly centrifuged five times. The resulting supernatant was centrifuged twice at 300×*g* for 10 min. PCs and NPCs were resuspended separately in ice-cold Hank's HEPES buffer (2 ml for PCs and 500 μl for NPCs) and luciferase activity of supernatant was measured. The cell numbers and viability were determined by the trypan blue exclusion method and the luciferase activity was normalized with respect to the number of cells.

Measurement of transaminase activity in serum

After transfection, the serum was collected from the anesthetized mice. Alanine aminotransferase (ALT/GPT) and aspartate aminotransferase (AST/GOT) activities in the serum were determined using Transaminase CII-Test Wako kit (Wako Pure Chemical Industries, Tokyo, Japan) according to manufacturer's instructions.

Quantification of luciferase mRNA in splenic CD11c$^+$ cells

At 6 hr after transfection, spleens were harvested and spleen cells were suspended in ice-cold RPMI-1640 medium on ice. Then, red blood cells were removed by incubation with hemolytic reagent (0.83% NH_4Cl solution) for 3 min at room temperature. CD11c$^+$ and CD11c$^-$ cells were separated by magnetic cell sorting with auto magnetic cell sorting (MACS) system (Miltenyi Biotec) following the manufacturer's instructions. Luciferase activity of each fraction was determined by luciferase assay. Total RNA was isolated from separated cells using GenElute Mammalian Total RNA Miniprep Kit (Sigma-Aldrich, St. Louis, MO). Reverse transcription of mRNA was carried out using PrimeScript® RT reagent Kit (Takara Bio, Shiga, Japan). Real-time polymerase chain reaction was performed using SYBR® Premix Ex Taq (Takara Bio) and Lightcycler Quick System 350S (Roche Diagnostics, Indianapolis, IN) with primers. The primers for luciferase and glyceraldehyde 3-phosphate dehydrogenase (GAPDH) cDNA were constructed as follows: primer for luciferase cDNA: 5′-TTCTTCGCCAAAAGCACTC-3′ (forward) and 5′-CCCTCGGGTGTAATCAGAAT-3′ (reverse); primer for GAPDH: 5′-TCTCCTGCGACTTCAACA-3′ (forward) and 5′-GCTGTAGCCGTATTCATTGT-3′ (reverse) (Sigma-Aldrich). The mRNA copy numbers were calculated for each sample from the standard curve using an instrument software ("Arithmetic Fit Point Analysis" for the Lightcycler). The results were expressed as relative copy numbers calculated relative to GAPDH mRNA (copy numbers of luciferase mRNA/copy numbers of GAPDH mRNA).

Statistical analysis

The results were expressed as the mean ± standard deviation of more than three experiments. Statistical analysis was performed using analysis of variance and the Turkey–Kramer test for multiple comparisons between groups or Student's *t*-test for two-group comparisons; $p < 0.05$ was considered statistically significant.

Results

Physicochemical properties of mannosylated lipoplexes and BLs

The physicochemical properties of DC-Chol:DOPE lipoplexes (bare lipoplexes), Man-C4-Chol:DOPE lipoplexes

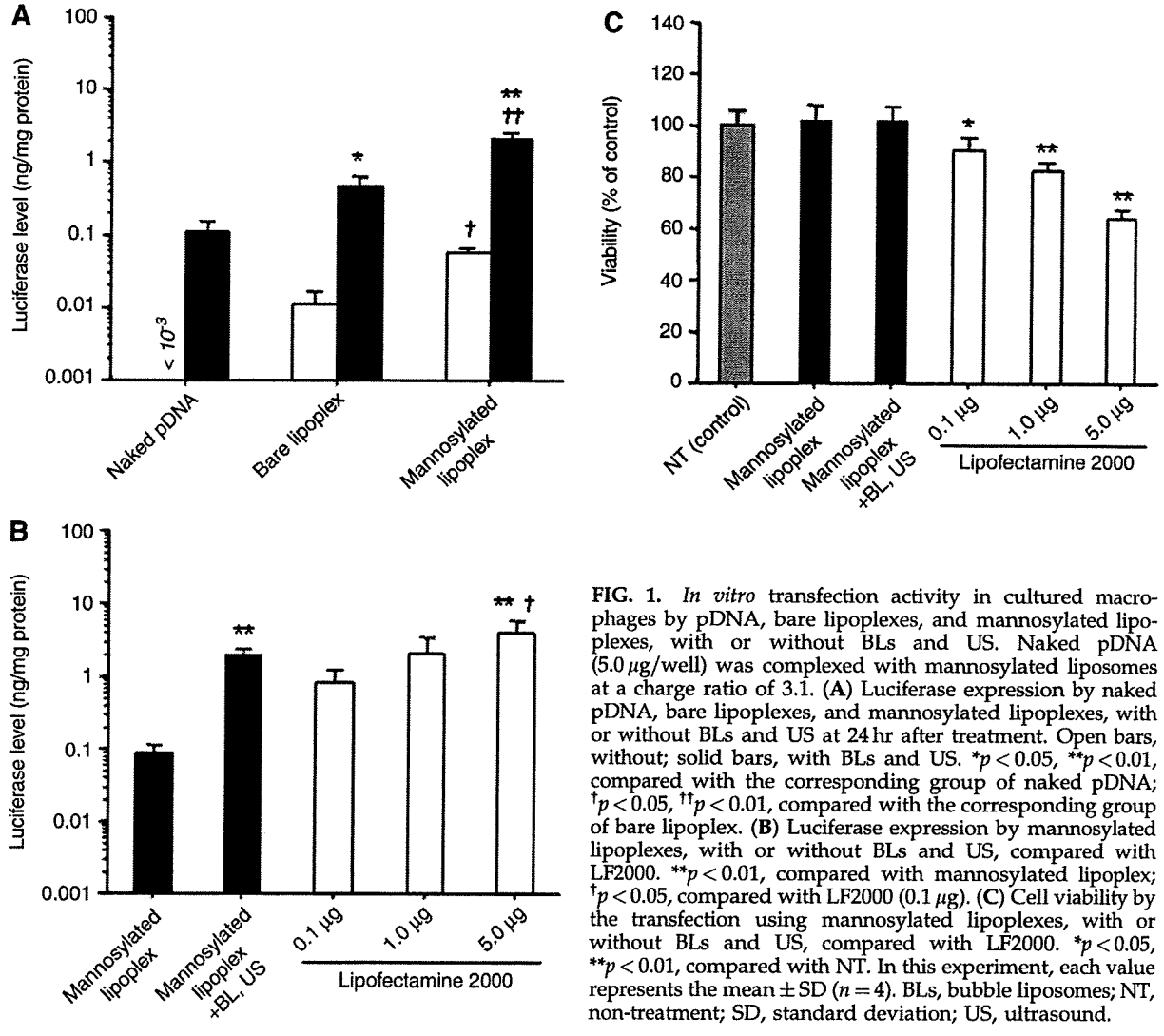

FIG. 1. *In vitro* transfection activity in cultured macrophages by pDNA, bare lipoplexes, and mannosylated lipoplexes, with or without BLs and US. Naked pDNA (5.0 μg/well) was complexed with mannosylated liposomes at a charge ratio of 3.1. (**A**) Luciferase expression by naked pDNA, bare lipoplexes, and mannosylated lipoplexes, with or without BLs and US at 24 hr after treatment. Open bars, without; solid bars, with BLs and US. $^{*}p < 0.05$, $^{**}p < 0.01$, compared with the corresponding group of naked pDNA; $^{\dagger}p < 0.05$, $^{\dagger\dagger}p < 0.01$, compared with the corresponding group of bare lipoplex. (**B**) Luciferase expression by mannosylated lipoplexes, with or without BLs and US, compared with LF2000. $^{**}p < 0.01$, compared with mannosylated lipoplex; $^{\dagger}p < 0.05$, compared with LF2000 (0.1 μg). (**C**) Cell viability by the transfection using mannosylated lipoplexes, with or without BLs and US, compared with LF2000. $^{*}p < 0.05$, $^{**}p < 0.01$, compared with NT. In this experiment, each value represents the mean ± SD ($n = 4$). BLs, bubble liposomes; NT, non-treatment; SD, standard deviation; US, ultrasound.

(mannosylated lipoplexes), and BLs used for all experiments were evaluated by measuring particle sizes and zeta potentials. The mean particle sizes of bare lipoplexes, mannosylated lipoplexes, and BLs were 123 ± 6.0, 128 ± 9.5, and 498 ± 18 nm ($n = 3$), respectively. Moreover, zeta potentials of bare lipoplexes, mannosylated lipoplexes, and BLs were 47.5 ± 1.4, 46.7 ± 3.8, and 0.08 ± 0.2 mV ($n = 3$), respectively. These values of mannosylated lipoplexes were the same as in our previous report (Hattori *et al.*, 2006a) and the particle size of BLs was almost identical to that in a previous report (Suzuki *et al.*, 2008).

Transfection efficiency in cultured mouse peritoneal macrophages

The transfection efficiency of mannosylated lipoplexes and BLs with US was significantly higher than that of naked pDNA or bare lipoplexes and BLs with US in cultured macrophages (Fig. 1A). The transfection efficiency of the combination of mannosylated lipoplexes and BLs was comparable to LF2000 (Fig. 1B). Then, we examined the cytotoxicity of this transfection method by mannosylated lipoplexes and BLs with US. As shown in Fig. 1C, this combination method did not exhibit any cytotoxic effect. However, LF2000 exhibited severe cytotoxic effects.

Intracellular uptake of pDNA in cultured mouse peritoneal macrophages

As shown in Fig. 2, the intracellular uptake of rhodamine-labeled pDNA was significantly increased by the combination method using mannosylated lipoplexes and BLs, compared with transfection by mannosylated lipoplexes. In contrast, the intracellular uptake of mannosylated liposomes by this combination method was smaller than that by transfection using mannosylated lipoplexes. This result means that extracellular mannosylated liposomes are disrupted by the cavitation energy generated by the collapse of BLs following US exposure, and thus, only pDNA carried by mannosylated liposomes is introduced into cells.

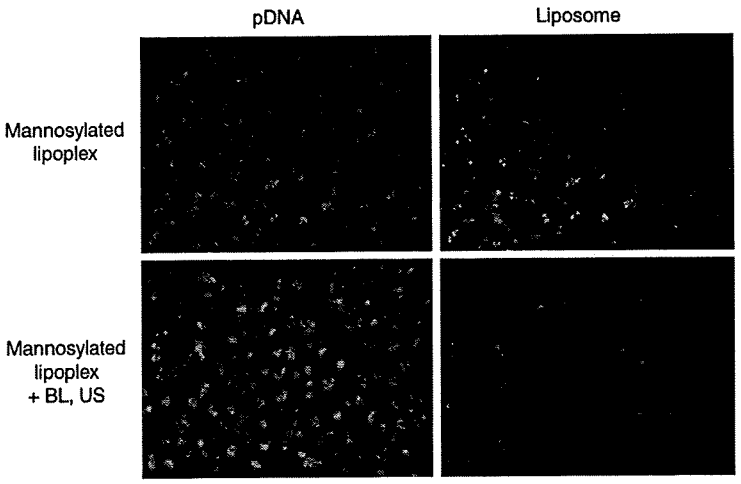

FIG. 2. Amount of intracellular uptake of naked pDNA and mannosylated liposomes in cultured macrophages. pDNA (red): TM-rhodamine-labeled pCMV-Luc; liposome (green): mannosylated liposome containing NBD-labeled phospholipids. Microscopy images were recorded 6 hr after the transfection using mannosylated lipoplexes, with or without BLs and US.

Transfection activities after intravenous administration in mice

The transfection efficiency by this combination method was higher than that by naked pDNA or bare lipoplexes and BLs using US in the liver and spleen (Fig. 3). The transfection efficiency by this combination method remained higher than that by mannosylated lipoplexes for 48 hr in the liver and spleen (Fig. 4). Moreover, as shown in Fig. 5, the increase of transfection efficiency by this combination method was not observed in the lung, kidney, and heart.

Intrahepatic transfection characteristics and hepatic toxicity after treatment

After transfection by this combination method using mannosylated lipoplexes and BLs with US, the gene expression in NPCs was significantly higher than that in PCs (Fig. 6A). This difference in gene expression between NPCs and PCs was similar to that obtained by treatment with mannosylated lipoplexes, but the gene expression in NPCs and PCs was higher than that obtained by treatment with mannosylated lipoplexes. On the other hand, the gene expression in NPCs and PCs was almost the same after treatment by naked pDNA and BLs with US. Further, we examined ALT and AST activities in the serum to investigate the hepatic toxicity after treatment by mannosylated lipoplexes and BLs using US. The ALT and AST activities following transfection by the combination method using mannosylated lipoplexes and BLs with US were almost the same as those following transfection using mannosylated lipoplexes (Fig. 6B).

Intrasplenic transfection characteristics after treatment

As shown in Fig. 7A, no luciferase activity in the splenic $CD11c^+$ and $CD11c^-$ cells at 10^7 cells was detected using mannosylated lipoplexes. However, with the combination method using mannosylated lipoplexes and BLs, the luciferase activity in the splenic $CD11c^+$ and $CD11c^-$ cells at 10^7 cells was significantly increased, and that in $CD11c^+$ cells, known as dendritic cells, was significantly higher than that in $CD11c^-$ cells. Moreover, comparable results were obtained from the experiment involving luciferase mRNA expression (Fig. 7B).

Transfection activities after direct exposure of liver or spleen to US

We investigated gene expression by directly exposing liver or spleen to US after intravenous administration of mannosylated lipoplexes and BLs. As shown in Fig. 8, direct exposure of liver or spleen to US after intravenous administration of BLs results in transfection of the US-exposed organ selectively.

Discussion

In this study, using mannosylated liposomes as a carrier of pDNA for controlling the kinetics of pDNA and optimizing the targeting properties, we tried to increase selectively the gene transfection efficiency in the targeted organ or the targeted cell by combining with BLs. Initially, we considered that the *in vitro* gene transfection efficiency in cultured macrophages, which are known for the expression of mannose receptors, was increased by using BLs and mannosylated lipoplexes as a carrier of pDNA, compared with the transfection using naked pDNA which is the conventional method, or the transfection using bare lipoplexes, which are nontargeted liposomes, as a carrier of pDNA. As shown in Figs. 1A and 2, significantly higher transfection efficiency in cultured macrophages was observed by the transfection using mannosylated lipoplexes and BLs, compared with the transfection using naked pDNA or bare lipoplexes and BLs with US. As this result shows that gene transfection efficiency was increased not only by the improvement of interaction with cell membrane by cationic carriers, but also by the improvement of interaction with mannose receptors by mannose modification, targeted cell-selective and efficient gene transfection is possible by this transfection method

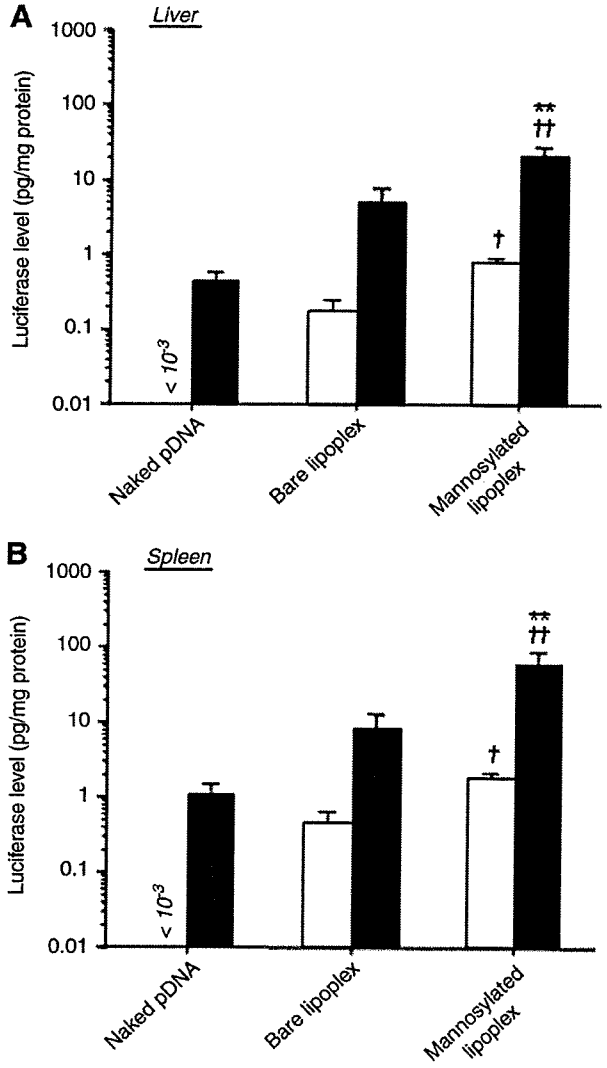

FIG. 3. Luciferase expression in the liver (A) and spleen (B) at 6 hr after the transfection by intravenous administration of naked pDNA, bare lipoplexes, and mannosylated lipoplexes, with or without BLs and US in mice. Open bars, without; solid bars, with BLs and US. Naked pDNA (50 μg) was complexed with mannosylated liposomes at a charge ratio of 3:1. Each value represents the mean $\pm$ SD ($n = 4$). $^{**}p < 0.01$, compared with the corresponding group of naked pDNA; $^{\dagger}p < 0.05$, $^{\dagger\dagger}p < 0.01$, compared with the corresponding group of bare lipoplex.

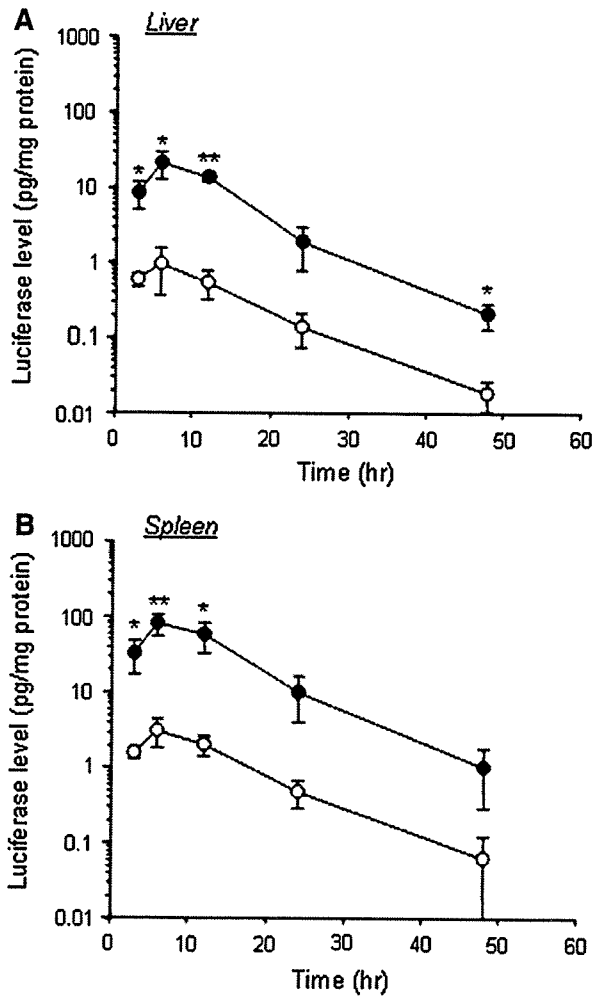

FIG. 4. Time-course of luciferase expression in the liver (A) and spleen (B) after transfection by intravenous administration of mannosylated lipoplexes, with or without BLs and US in mice. Open circles, without; solid circles, with BLs and US. Each value represents the mean $\pm$ SD ($n = 4$). $^{*}p < 0.05$, $^{**}p < 0.01$, compared with or without BLs and US.

using mannosylated lipoplexes and BLs with US. Then we found that the transfection efficiency of this combination method using US was the same as that of LF2000, which is used widely as an efficient transfection reagent (Fig. 1B). Moreover, the cytotoxicity of this combination method using US was significantly lower than that of LF2000 (Fig. 1C). In addition, as shown in Fig. 2, although intracellular uptake of pDNA into macrophages was increased by this combination method, intracellular uptake of mannosylated liposomes was low; therefore, different transfection mechanisms based on intracellular uptake of pDNA via endocytosis were observed by the transfection using lipoplexes. This result may indicate that BLs and US are operated on mannosylated lipoplexes existing on the cell surface, and then pDNA is introduced directly into the cytoplasm. It is generally considered that gene transfection into APCs such as macrophages is difficult (Erbacher *et al.*, 1996; Sakurai *et al.*, 2000). However, in this study, we demonstrated that this combination method using mannosylated lipoplexes and BLs with US could achieve significantly high transfection efficiency in primary cultured peritoneal macrophages.

To achieve effective cancer vaccine therapy, it is necessary to transfect the antigen-presenting gene efficiently into the APCs, such as macrophages and dendritic cells distributed in the liver and spleen (Goerdt *et al.*, 1999; Melief, 2008). Especially, dendritic cells are major target cells for DNA vaccine therapy. As the number of APCs in the spleen is extremely low, it is difficult to transfect the pDNA selectively

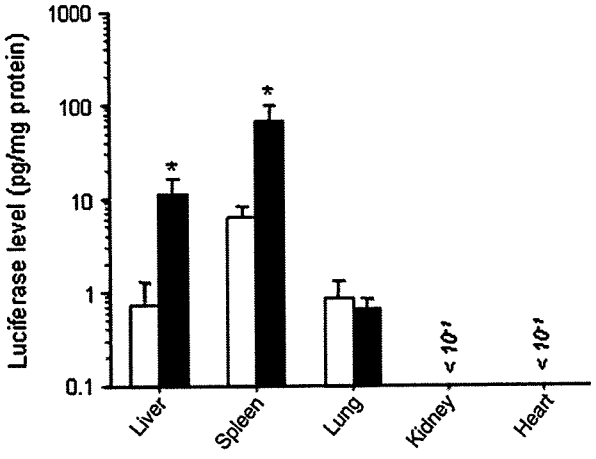

FIG. 5. Luciferase expression in each organ after transfection by intravenous administration of mannosylated lipoplexes, with or without BLs and US in mice. Open bars, without; solid bars, with BLs and US. Each value represents the mean ± SD ($n = 4$). *$p < 0.05$, compared with or without BLs and US.

into macrophages and dendritic cells. We showed that the *in vivo* selective gene transfection efficiency into mannose receptor-expressing cells in the liver and spleen could be increased by this combination method using US. In this study, US was applied externally using a large probe with diameter 20 mm (see Materials and Methods section). As shown in Figs. 3 and 4, the gene transfection efficiency in the liver and spleen was significantly increased by using mannosylated lipoplexes, compared with transfection using naked pDNA or bare lipoplexes and BLs with US. We have already reported that mannosylated lipoplexes used in this study were accumulated in the liver and spleen, compared with bare lipoplexes (Yamada *et al.*, 2004). Therefore, these results show that *in vivo* distribution characteristics of carriers are important for enhancement of gene transfection efficiency in the targeted organ by using BLs. Moreover, to investigate the cellular localization of gene expression after transfection by the combination of mannosylated lipoplexes and BLs with US, the gene expression levels of NPCs in the liver and dendritic cells in the spleen were determined. As a result, we demonstrated that this combination method could transfect the gene selectively into hepatic NPCs and splenic dendritic cells (Figs. 6A and 7). The gene transfection efficiency into splenic dendritic cells could be monitored by the luciferase protein in this combination method using US (Fig. 7), whereas a previous study by our group was only able to detect the luciferase mRNA in the transfection method using mannosylated lipoplexes (Hattori *et al.*, 2006b). Therefore, this combination method using US results in high gene transfection efficiency in splenic dendritic cells. Moreover, there was very little *in vitro* cytotoxicity and hepatic toxicity in mice, using this method (Figs. 1C and 6B). Therefore, this transfection method may be more suitable for clinical application. These results indicate that the combination of mannosylated lipoplexes and BLs with US is a novel method for markedly increasing gene expression in hepatic NPCs and splenic dendritic cells following intravenous injection in mice.

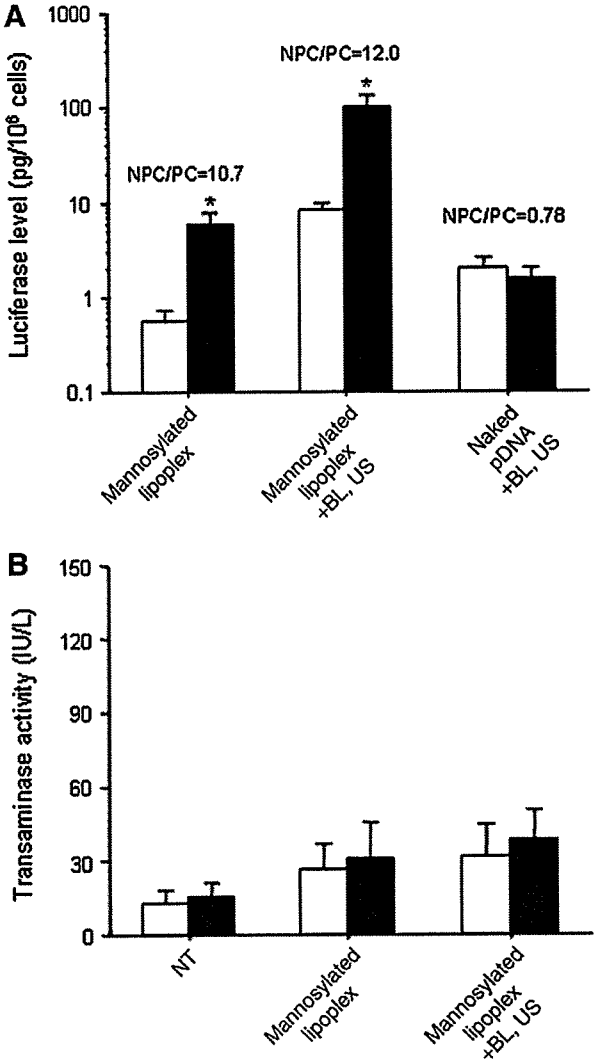

FIG. 6. (A) Hepatic cellular localization of luciferase expression after intravenous administration of naked pDNA or mannosylated lipoplexes, with or without BLs and US in mice. Luciferase expression of PC (open bars) and NPC (solid bars) was measured at 6 hr after transfection. *$p < 0.05$, compared with PC. Each value represents the mean ± SD ($n = 3$). (B) Serum transaminase activity after the transfection using mannosylated lipoplexes with or without BLs and US in mice. Transaminase activities of ALT (open bars) and AST (solid bars) were measured at 6 hr after transfection. Each value represents the mean ± SD ($n = 4$). NPCs, nonparenchymal cells; PCs, parenchymal cells.

In this study, although US was applied externally for the experiment involving noninvasive conditions, the increase of gene expression by the combination of mannosylated lipoplexes and BLs with US was observed in the liver and spleen, but not in the lung, kidney, and heart (Fig. 5). Although the uptake into the reticuloendothelial system (RES) can be avoided by PEGylation of the liposomes, large amounts of PEGylated liposomes are distributed in the liver and spleen (Elbayoumi and Torchilin, 2006). Moreover, it is known

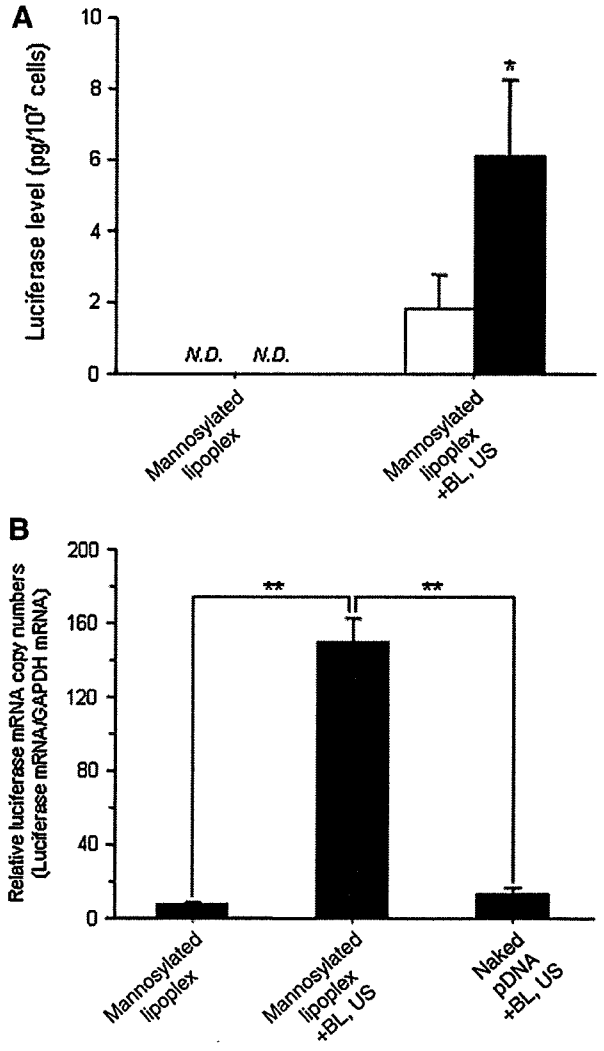

FIG. 7. Luciferase expression and luciferase mRNA expression in mouse splenic CD11c$^+$ cells after intravenous administration of naked pDNA or mannosylated lipoplexes, with or without BLs and US at 6 hr after transfection. (**A**) Luciferase activity was measured in splenic CD11c$^-$ (open bar) or CD11c$^+$ (solid bar) cells. $^*p < 0.05$, compared with CD11c$^-$ cells. (**B**) Luciferase mRNA and GAPDH mRNA eluted from CD11c$^+$ cells were measured by quantitative reverse transcription-polymerase chain reaction (RT-PCR). $^{**}p < 0.01$, compared with mannosylated lipoplex +BL, US. In this experiment, each value represents the mean ± SD ($n = 3$). GAPDH, glyceraldehyde 3-phosphate dehydrogenase.

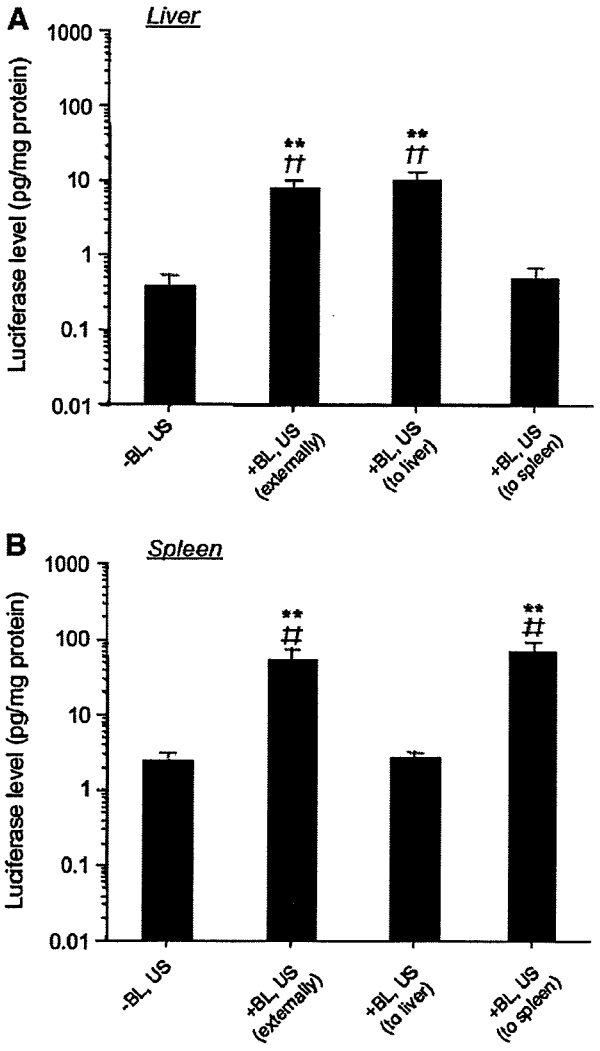

FIG. 8. Luciferase expression by mannosylated lipoplexes and BLs with US exposure externally or directly. Luciferase expression in the liver (**A**) and spleen (**B**) at 6 hr after the transfection by intravenous administration of mannosylated lipoplexes, with or without BLs and US, in mice. Each value represents the mean ± SD ($n = 4$). $^{**}p < 0.01$, compared with the corresponding group of −BL, US; $^{††}p < 0.01$, compared with the corresponding group of +BL, US (to spleen); $^{‡‡}p < 0.01$, compared with the corresponding group of +BL, US (to liver).

that PEGylated liposomes with a particle size over 500 nm are easily taken up into the RES, compared with smaller conventional liposomes (Ishida *et al.*, 1999). Harashima *et al.* (1994) also reported a similar effect of particle size on the distribution of liposomes. The BLs used in this study possesses a particle size of approximately 500 nm, which would be preferentially taken up by the RES as suggested by these reports (Harashima *et al.*, 1994; Ishida *et al.*, 1999). Considering that the RES comprises Kupffer cells and splenic macrophages/dendritic cells which express mannose receptors, the treatment of mannosylated lipoplexes is quite reasonable (Fig. 5). On the other hand, the observation that treatment with BLs and US was not effective in the lung, kidney, and heart (Fig. 5) agrees in part with the study by Negishi *et al.* (2008) and Chen *et al.* (2006), who reported that gene transfection in the kidney was difficult in a treatment using microbubbles. Therefore, these observations support our finding that the combination method using mannosylated lipoplexes and BLs with US offers important advantages for gene transfection into mannose receptor-expressing cells in the RES.

In the experiments, we applied US externally using a comparatively large probe in mice (diameter, 20 mm) to evaluate the gene transfection efficiency in noninvasive conditions. Consequently, the organ specificity of the gene expression was characterized (Fig. 5). As the US-exposed organ-specific gene expression was observed by direct exposure of the organ to US (Fig. 8), more effective gene transfection into the targeted organ was also possible by this transfection method using mannosylated lipoplexes and BLs with US.

To date, nucleic acid introduction methods using microbubbles such as BLs have been applied in *in vitro* using not only naked pDNA but also naked siRNA and oligodeoxynucleotides (Haag *et al.*, 2006; Negishi *et al.*, 2008). However, it may be difficult to use these materials in *in vivo* because of the poor stability of naked nucleic acids in blood. The major feature of the combination method using mannosylated lipoplexes and BLs with US was to both improve the pDNA stability in the body and control the kinetics of pDNA by using lipoplexes. As the mannosylated liposomes used in this study can form complexes with different nucleic acids via electrostatic interaction, this transfection method can be applied to many types of diseases. We have reported that mannosylated liposomes/nuclear factor κB complexes could significantly suppress hepatitis (Higuchi *et al.*, 2006; Huang *et al.*, 2009). Therefore, in the future, the combination method using mannosylated liposomes/various types of nucleic acids and BLs with US would be widely applied using mannose receptor-expressing cells for a variety of genetic diseases.

In conclusion, we demonstrated that the gene transfection efficiency in macrophages and dendritic cells was significantly increased by the combination method using mannosylated lipoplexes and BLs with US. To date, various targeting ligands for cell-selective targeting, such as galactose (Fumoto *et al.*, 2004; Letrou-Bonneval *et al.*, 2008), folic acid (Zuber *et al.*, 2003; Fernandes *et al.*, 2008), anisamide (Li *et al.*, 2008), hyaluronan (Eliaz and Szoka, 2001), RGD peptide (Anwer *et al.*, 2004; Oba *et al.*, 2008), IRQ peptide (Mudhakir *et al.*, 2008), and anti-Her2 antibody (Chiu *et al.*, 2004; Strehblow *et al.*, 2005), have been reported. Therefore, these observations would be valuable for the development of cell-selective gene delivery systems by using various ligand-modified lipoplexes and BLs with US.

Acknowledgment

This work was supported in part by a grant-in-aid for scientific research from the Ministry of Education, Culture, Sports, Science, and Technology of Japan, and by Health and Labour Sciences Research Grants for Research on Advanced Medical Technology from the Ministry of Health, Labour, and Welfare of Japan.

Disclosure Statement

No competing financial interests exist.

References

Anwer, K., Kao, G., Rolland, A., Driessen, W.H., and Sullivan, S.M. (2004). Peptide-mediated gene transfer of cationic lipid/plasmid DNA complexes to endothelial cells. J. Drug Target. 12, 215–221.

Chen, S., Ding, J.H., Bekeredjian, R., Yang, B.Z., Shohet, R.V., Johnston, S.A., Hohmeier, H.E., Newgard, C.B., and Grayburn, P.A. (2006). Efficient gene delivery to pancreatic islets with ultrasonic microbubble destruction technology. Proc. Natl. Acad. Sci. U.S.A. 103, 8469–8474.

Chiu, S.J., Ueno, N.T., and Lee, R.J. (2004). Tumor-targeted gene delivery via anti-HER2 antibody (trastuzumab, Herceptin) conjugated polyethylenimine. J. Controlled Release 97, 357–369.

Elbayoumi, T.A., and Torchilin, V.P. (2006). Enhanced accumulation of long-circulating liposomes modified with the nucleosome-specific monoclonal antibody 2C5 in various tumours in mice: Gamma-imaging studies. Eur. J. Nucl. Med. Mol. Imaging 33, 1196–1205.

Eliaz, R.E., and Szoka, F.C., Jr. (2001). Liposome-encapsulated doxorubicin targeted to CD44: A strategy to kill CD44-overexpressing tumor cells. Cancer Res. 61, 2592–2601.

Erbacher, P., Bousser, M.T., Raimond, J., Monsigny, M., Midoux, P., and Roche, A.C. (1996). Gene transfer by DNA/glycosylated polylysine complexes into human blood monocyte-derived macrophages. Hum. Gene Ther. 7, 721–729.

Fernandes, J.C., Wang, H., Jreyssaty, C., Benderdour, M., Lavigne, P., Qiu, X., Winnik, F.M., Zhang, X., Dai, K., and Shi, Q. (2008). Bone-protective effects of nonviral gene therapy with folate-chitosan DNA nanoparticle containing interleukin-1 receptor antagonist gene in rats with adjuvant-induced arthritis. Mol. Ther. 16, 1243–1251.

Fumoto, S., Kawakami, S., Ito, Y., Shigeta, K., Yamashita, F., and Hashida, M. (2004). Enhanced hepatocyte-selective *in vivo* gene expression by stabilized galactosylated liposome/plasmid DNA complex using sodium chloride for complex formation. Mol. Ther. 10, 719–729.

Gersting, S.W., Schillinger, U., Lausier, J., Nicklaus, P., Rudolph, C., Plank, C., Reinhardt, D., and Rosenecker, J. (2004). Gene delivery to respiratory epithelial cells by magnetofection. J. Gene Med. 6, 913–922.

Goerdt, S., Politz, O., Schledzewski, K., Birk, R., Gratchev, A., Guillot, P., Hakiy, N., Klemke, C.D., Dippel, E., Kodelja, V., and Orfanos, C.E. (1999). Alternative versus classical activation of macrophages. Pathobiology 67, 222–226.

Haag, P., Frauscher, F., Gradl, J., Seitz, A., Schäfer, G., Lindner, J.R., Klibanov, A.L., Bartsch, G., Klocker, H., and Eder, I.E. (2006). Microbubble-enhanced ultrasound to deliver an antisense oligodeoxynucleotide targeting the human androgen receptor into prostate tumours. J. Steroid Biochem. Mol. Biol. 102, 103–113.

Harashima, H., Sakata, K., Funato, K., and Kiwada, H. (1994). Enhanced hepatic uptake of liposomes through complement activation depending on the size of liposomes. Pharm. Res. 11, 402–406.

Hattori, Y., Kawakami, S., Suzuki, S., Yamashita, F., and Hashida, M. (2004). Enhancement of immune responses by DNA vaccination through targeted gene delivery using mannosylated cationic liposome formulations following intravenous administration in mice. Biochem. Biophys. Res. Commun. 317, 992–999.

Hattori, Y., Kawakami, S., Lu, Y., Nakamura, K., Yamashita, F., and Hashida, M. (2006a). Enhanced DNA vaccine potency by mannosylated lipoplex after intraperitoneal administration. J. Gene Med. 8, 824–834.

Hattori, Y., Kawakami, S., Nakamura, K., Yamashita, F., and Hashida, M. (2006b). Efficient gene transfer into macrophages and dendritic cells by *in vivo* gene delivery with mannosylated

lipoplex via the intraperitoneal route. J. Pharmacol. Exp. Ther. 318, 828–834.
Higuchi, Y., Kawakami, S., Oka, M., Yabe, Y., Yamashita, F., and Hashida, M. (2006). Intravenous administration of mannosylated cationic liposome/NFκB decoy complexes effectively prevent LPS-induced cytokine production in a murine liver failure model. FEBS Lett. 580, 3706–3714.
Huang, H., Sakurai, F., Higuchi, Y., Kawakami, S., Hashida, M., Kawabata, K., and Mizuguchi, H. (2009). Suppressive effects of sugar-modified cationic liposome/NF-κB decoy complexes on adenovirus vector-induced innate immune responses. J. Controlled Release 133, 139–145.
Ishida, O., Maruyama, K., Sasaki, K., and Iwatsuru, M. (1999). Size-dependent extravasation and interstitial localization of polyethyleneglycol liposomes in solid tumor-bearing mice. Int. J. Pharm. 190, 49–56.
Iwanaga, K., Tominaga, K., Yamamoto, K., Habu, M., Maeda, H., Akifusa, S., Tsujisawa, T., Okinaga, T., Fukuda, J., and Nishihara, T. (2007). Local delivery system of cytotoxic agents to tumors by focused sonoporation. Cancer Gene Ther. 14, 354–363.
Kawakami, S., Sato, A., Nishikawa, M., Yamashita, F., and Hashida, M. (2000). Mannose receptor-mediated gene transfer into macrophages using novel mannosylated cationic liposomes. Gene Ther. 7, 292–299.
Kim, C.Y., Kang, E.S., Kim, S.B., Kim, H.E., Choi, J.H., Lee, D.S., Im, S.J., Yang, S.H., Sung, Y.C., Kim, B.M., and Kim, B.G. (2008). Increased *in vivo* immunological potency of HB-110, a novel therapeutic HBV DNA vaccine, by electroporation. Exp. Mol. Med. 40, 669–676.
Kobayashi, N., Nishikawa, M., Hirata, K., and Takakura, Y. (2004). Hydrodynamics-based procedure involves transient hyperpermeability in the hepatic cellular membrane: Implication of a nonspecific process in efficient intracellular gene delivery. J. Gene Med. 6, 584–592.
Letrou-Bonneval, E., Chèvre, R., Lambert, O., Costet, P., André, C., Tellier, C., and Pitard, B. (2008). Galactosylated multimodular lipoplexes for specific gene transfer into primary hepatocytes. J. Gene Med. 10, 1198–1209.
Li, S.-D., Chono, S., and Huang, L. (2008). Efficient gene silencing in metastatic tumor by siRNA formulated in surface-modified nanoparticles. J. Controlled Release 126, 77–84.
Melief, C.J. (2008). Cancer immunotherapy by dendritic cells. Immunity 29, 372–383.
Mudhakir, D., Akita, H., Tan, E., and Harashima, H. (2008). A novel IRQ ligand-modified nano-carrier targeted to a unique pathway of caveolar endocytic pathway. J. Controlled Release 125, 164–173.
Negishi, Y., Endo, Y., Fukuyama, T., Suzuki, R., Takizawa, T., Omata, D., Maruyama, K., and Aramaki, Y. (2008). Delivery of siRNA into the cytoplasm by liposomal bubbles and ultrasound. J. Controlled Release 132, 124–130.
Niidome, T., and Huang, L. (2002). Gene therapy progress and prospects: Nonviral vectors. Gene Ther. 9, 1647–1652.
Oba, M., Aoyagi, K., Miyata, K., Matsumoto, Y., Itaka, K., Nishiyama, N., Yamasaki, Y., Koyama, H., and Kataoka, K. (2008). Polyplex micelles with cyclic RGD peptide ligands and disulfide cross-links directing to the enhanced transfection via controlled intracellular trafficking. Mol. Pharm. 5, 1080–1092.
Sakurai, F., Inoue, R., Nishino, Y., Okuda, A., Matsumoto, O., Taga, T., Yamashita, F., Takakura, Y., and Hashida, M. (2000). Effect of DNA/liposome mixing ratio on the physicochemical characteristics, cellular uptake and intracellular trafficking of plasmid DNA/cationic liposome complexes and subsequent gene expression. J. Controlled Release 66, 255–269.
Scherer, F., Anton, M., Schillinger, U., Henke, J., Bergemann, C., Krüger, A., Gänsbacher, B., and Plank, C. (2002). Magnetofection: Enhancing and targeting gene delivery by magnetic force *in vitro* and *in vivo*. Gene Ther. 9, 102–109.
Shen, Z.P., Brayman, A.A., Chen, L., and Miao, C.H. (2008). Ultrasound with microbubbles enhances gene expression of plasmid DNA in the liver via intraportal delivery. Gene Ther. 15, 1147–1155.
Strehblow, C., Schuster, M., Moritz, T., Kirch, H.C., Opalka, B., and Petri, J.B. (2005). Monoclonal antibody-polyethyleneimine conjugates targeting Her-2/neu or CD90 allow cell type-specific nonviral gene delivery. J. Controlled Release 102, 737–747.
Suzuki, R., Takizawa, T., Negishi, Y., Utoguchi, N., Sawamura, K., Tanaka, K., Namai, E., Oda, Y., Matsumura, Y., and Maruyama, K. (2008). Tumor specific ultrasound enhanced gene transfer *in vivo* with novel liposomal bubbles. J. Controlled Release 125, 137–144.
Taylor, P.R., Gordon, S., and Martinez-Pomares, L. (2005). The mannose receptor: Linking homeostasis and immunity through sugar recognition. Trends Immunol. 26, 104–110.
Wijagkanalan, W., Higuchi, Y., Kawakami, S., Teshima, M., Sasaki, H., and Hashida, M. (2008). Enhanced anti-inflammation of inhaled dexamethasone palmitate using mannosylated liposomes in an endotoxin-induced lung inflammation model. Mol. Pharmacol. 74, 1183–1192.
Yamada, M., Nishikawa, M., Kawakami, S., Hattori, Y., Nakano, T., Yamashita, F., and Hashida, M. (2004). Tissue and intrahepatic distribution and subcellular localization of a mannosylated lipoplex after intravenous administration in mice. J. Controlled Release 98, 157–167.
Zuber, G., Zammut-Italiano, L., Dauty, E., and Behr, J.P. (2003). Targeted gene delivery to cancer cells: Directed assembly of nanometric DNA particles coated with folic acid. Ang. Chem. Int. Ed. 42, 2666–2669.

Address correspondence to:
Dr. Shigeru Kawakami
Department of Drug Delivery Research
Graduate School of Pharmaceutical Sciences
Kyoto University
46-29 Yoshida-shimoadachi-cho, Sakyo-ku
Kyoto 606-8501
Japan

E-mail: kawakami@pharm.kyoto-u.ac.jp

Received for publication June 18, 2009;
accepted after revision August 31, 2009.

Published online: December 17, 2009.

製剤技術
製剤と粒子設計

バブルリポソームの開発と遺伝子・ドラッグデリバリーシステムへの応用

Development of novel liposomal bubbles (Bubble liposomes) and its application to gene and drug delivery system

帝京大学 薬学部
鈴木 亮，小田雄介，丸山一雄
RYO SUZUKI, YUSUKE ODA, KAZUO MARUYAMA
Department of Biopharmaceutics, School of Pharmaceutical Sciences, Teikyo University

Recently, we developed novel liposomal bubbles (Bubble liposomes) containing the ultrasound imaging gas (perfluoropropane). These Bubble liposomes were about 500nm in diameter and induced cavitation by ultrasound exposure. Using this cavitation power, transient pores were provided on cell membrane without cytotoxicity. Then, extracellular molecules such as plasmid DNA, drug and antigen could be delivered into cytosol. In this review, we introduced about gene and antigen delivery system by the combination of Bubble liposomes and ultrasound.

はじめに

脂質二重膜からなる閉鎖小胞であるリポソームは，その内部への薬物の封入，表面への機能性高分子の付与やターゲティング分子として抗体やペプチドなどを容易に修飾可能であることから，薬物キャリアーとして期待されている。実際にTable 1に示すようなリポソーム製剤が世界中で上市されており，このリポソーム技術は薬物治療の最適化を目指すドラッグデリバリーシステム(DDS)のための製剤技術として注目されている。

そのなかで著者らは，リポソームに関する研究を長年続けており，がん細胞にアクティブターゲティング可能な抗がん剤封入リポソームや中性子補捉療法におけるがん組織へのボロン化合物送達システムとしてのリポソームの利用などさまざまなリポソーム開発に携わってきた[1~5]。そして最近では，新たな取り組みとしてリポソームの内水相部分に超音波造影ガスであるパーフルオロプロパンを封入した新たなタイプのリポソーム開発を行っている[6~10]。

そこで本稿では，著者らが開発を続けているリポソーム型微小気泡(バブルリポソーム)について紹介するとともに，その遺伝子・ドラッグデリバリーシステムへの応用の可能性について論じる。

Table 1 Liposomal product in the world

Brand Name	Drug	Lipid composition	Release Year World	Japan
AmBisome	Amphotericin B	HSPC/Chol/DSPG/α-tocopherol	1990	2006
DaunoXome	Daunorubicin	DSPC/Chol	1995	−
DOXIL/CAELYX	Doxorubicin	HSPC/Chol/MPEG-DSPE	1995	2007
Myocet	Doxorubicin	eggPC/Chol	1995	−
Visudyne	Verteporfin	eggPC/DMPC	2001	2004

リポソーム応用の新展開(NTS)p.637引用

1．バブルリポソームの特性

近年の超音波診断技術の進展は目覚しく，超音波造影装置の高解像度化や3D撮像などが可能となっている。これに加え，超音波造影剤の開発も進められており，本邦では世界に先駆け肝腫留性病変のための超音波造影剤であるSonazoidが上市された(Table 2)。このSonazoidは静脈内投与後，速やかに肝臓のクッパー細胞に取り込まれることで肝腫留病変を陰影像としてとらえることができる優れた超音波造影剤である。このように肝臓のク

＊本稿は，第24回製剤と粒子設計シンポジウム(2007年11月，浜松)での特別講演をまとめたものである。
＊本欄は，製剤と粒子設計部会の編集企画によるものである。

Table 2 Microbubbles and Bubble liposomes

Brand Name	Shell	Entrapping gas	Country	Size (μm)
Levovist	Galactose	Air	EU, JP	2~4
Optison	Albumin	Perfluoropropane	US, EU	3~32
Definity	Lipids	Perfluoropropane	US	1.1~20
Imagent	Lipids	Perfluoropropane	US	5
Sonovue	Lipids	Sulforhexafluoride	EU	2.5
Sonazoid	Lipids	Perfluorobutane	JP	2~3
Bubble liposomes	Liposome	Perfluoropropane	—	0.4~0.9

生体医工学43(2), 212(2005), 微細気泡の最新技術(2006)から一部抜粋

ッパー細胞を利用した超音波造影が可能になるのは，Sonazoidがホスファチジルセリンを殻にもつ気泡であること，さらに粒子サイズが2～3 μmでありクッパー細胞に積極的に貪食されやすい性質を有しているためである(**Fig. 1 (a)**)[11]。

一方，われわれが開発したバブルリポソームは，粒子サイズが約500nmであり，電子顕微鏡により粒子構造を確認したところ脂質二重膜(リポソーム構造)内に気泡が存在したユニークな構造であることが判明した(**Fig. 1 (c)**)。このバブルリポソームはSonazoid（**Fig. 1 (b)**）より小さい上，ポリエチレングリコール(PEG)修飾リポソーム内に気泡が封入された構造であるため表面に存在するPEGの影響でクッパー細胞による貪食から逃れやすくなっている。したがって，粒子サイズおよびクッパー細胞による貪食の回避などの観点から，バブルリポソームが組織深部にまで到達可能になるものと期待される。

前述のようにバブルリポソームには，超音波造影ガスとしてパーフルオロプロパンが封入されているため，超音波造影剤として機能しうると考えられる。そこで，超音波造影装置を用いてバブルリポソームの撮像を試みたところ，バブルリポソームによるエコーシグナルの増強が観察された(**Fig. 2 (a)**)。一方，ガス未封入のPEG-リポソームでは，エコーシグナルの増強は観察されなかった。次に，このバブルリポソームをマウス尾静脈から全身投与し，心臓の超音波造影を行った。その結果，バブルリポソーム投与群で，心臓内腔のエコーシグナルの増強が認められた(**Fig. 2 (b)**)。これは，全身循環するバブルリポソームが造影されたものと考えられた。このように，バブルリポソームが*in vivo*における超音波造影剤としても利用可能になると期待される。

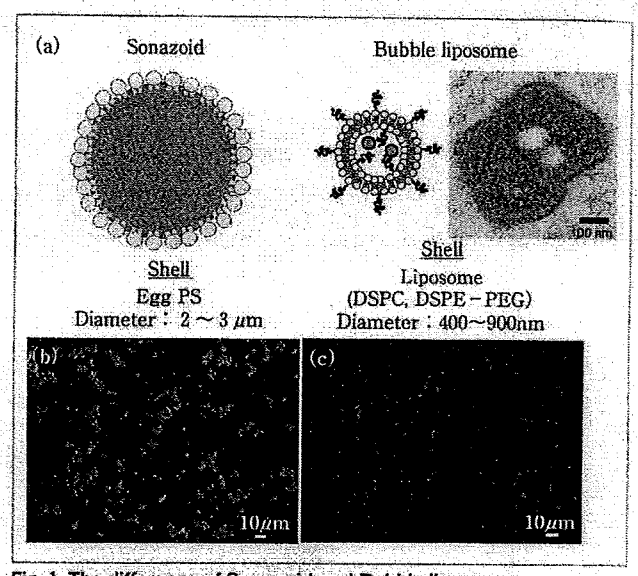

Fig. 1 The difference of Sonazoid and Bubble liposomes
(a) Characters of Sonazoid and Bubble liposomes
Microscopy of (b) Sonazoid and (c) Bubble liposomes
PS : Phosphatidylserine, DSPC : Distearoylphosphatidylcholine, DSPE-PEG : 1,2-distearoyl-sn-glycero-3-phophatidylethanolamine s-methoxypolyethyleneglycol

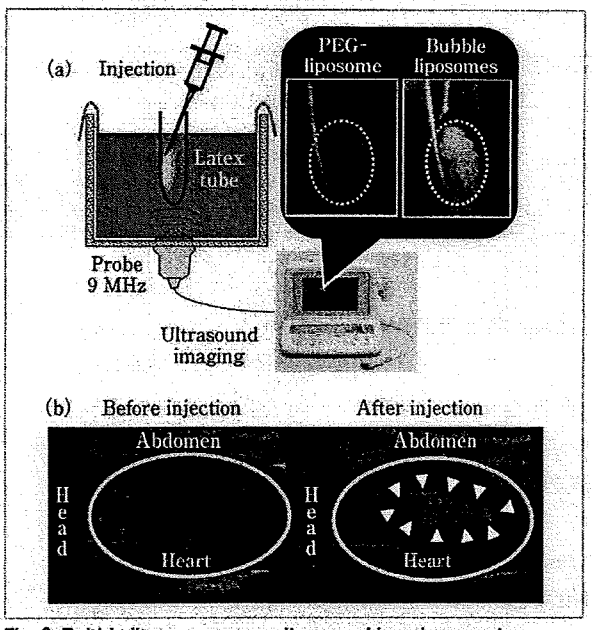

Fig. 2 Bubble liposomes as a ultrasound imaging agent
(a) Ultrasound imaging of PEG-liposome and Bubble liposomes *in vitro*
(b) Sonography of heart using Bubble liposomes

2．バブルリポソームと超音波照射の併用による遺伝子デリバリー

超音波造影で一般的に利用される周波数とは異なる低

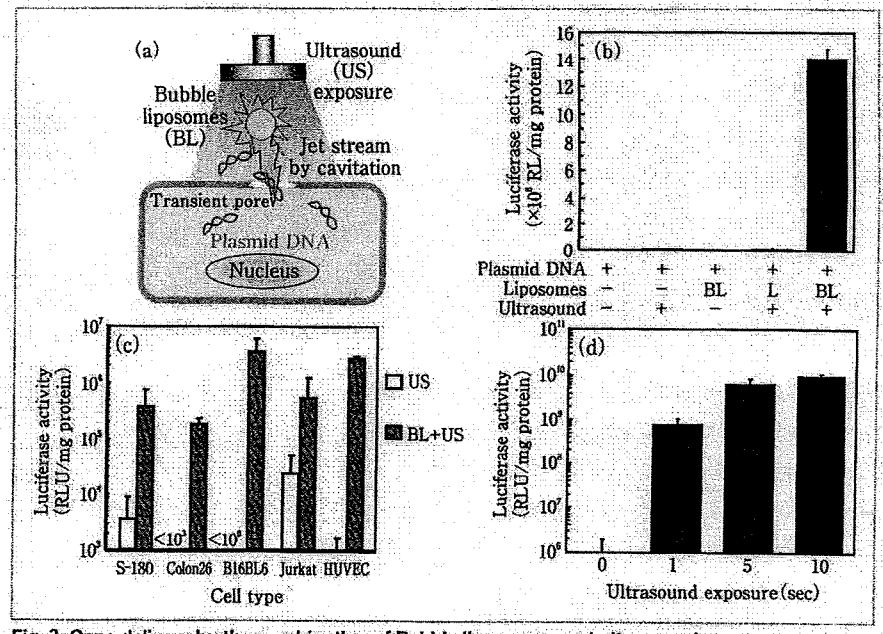

Fig. 3 Gene delivery by the combination of Bubble liposomes and ultrasound

(a) Schema of gene delivery mechanism

(b) Luciferase cording plasmid DNA delivery into COS-7 cells using Bubble liposomes and/or ultrasound

(c) Luciferase cording plasmid DNA delivery into various types of cell
Each cell (1×10^5 cells/500μL) was mixed with pCMV-Luc (5μg) and Bubble liposomes (60μg). The cell mixture was exposed to ultrasound (frequency : 2 MHz, duty : 50%, burst rate : 2 Hz, intensity : 2.5 W/cm², time : 10 sec.)

(d) Effect of ultrasound exposure time on gene delivery COS-7 cells (1×10^5 cells/500μL) were mixed with pCMV-Luc (5μg) and Bubble liposomes (60μg). The cell mixture was exposed to ultrasound (b) : (frequency : 2 MHz, duty : 50%, burst rate : 2 Hz, intensity : 2.5W/cm², time : 10sec.) or (c) : (frequency : 2 MHz, duty : 50%, burst rate : 2 Hz, intensity : 2.5W/cm², time : 0~10 sec.). The cells were washed and cultured for 2 days, then luciferase activity was determined.

い周波数帯の超音波をバブルリポソームに照射すると効率よくバブルリポソームのキャビテーション(空洞現象)が誘導される。キャビテーションとは，液体に超音波を照射したときの負の圧力が液体を維持するのに必要な圧力に打ち勝ったときに空洞を生じる現象である。このキャビテーション気泡は最終的に圧壊するが，この圧壊時に気泡近傍にジェット流が生じることが知られている。この現象を利用すると細胞膜に一過性の穴を開けることができ，その穴から細胞内にプラスミドDNAなどの外来性遺伝子や薬物などを送達することが可能である(**Fig.3(a)**)。

そこで，バブルリポソームと超音波照射の併用による遺伝子導入について検討した。その結果，バブルリポソームと超音波照射を併用したときのみ高い遺伝子発現が確認され，バブルリポソームと超音波の併用により効率よく細胞内に遺伝子が導入されていることが示された(**Fig. 3 (b)**)。さらに，さまざまな種類の細胞にルシフェラーゼ発現プラスミドDNAをバブルリポソームと超音波照射の併用より遺伝子導入したところ，いずれの細胞種においても超音波照射単独による遺伝子導入より高いルシフェラーゼ発現が認められた(**Fig. 3 (c)**)。

このようにバブルリポソームと超音波の併用が細胞種を問わず遺伝子導入可能であったのは，キャビテーションによる物理的エネルギーを利用して細胞質内に遺伝子を直接導入できるためであると考えられた。さらに，本方法の特徴としてあげられるのが，非常に短時間に遺伝子導入が完了することにある。実際に超音波照射時間と遺伝子導入活性を評価したところ，超音波照射がわずか1秒でも遺伝子発現が認められており，本方法が瞬時に遺伝子を細胞内に導入可能であることが示された(**Fig. 3 (d)**)。このように，本方法は瞬時に遺伝子導入可能であるため，血流があり既存の非ウイルスベクター

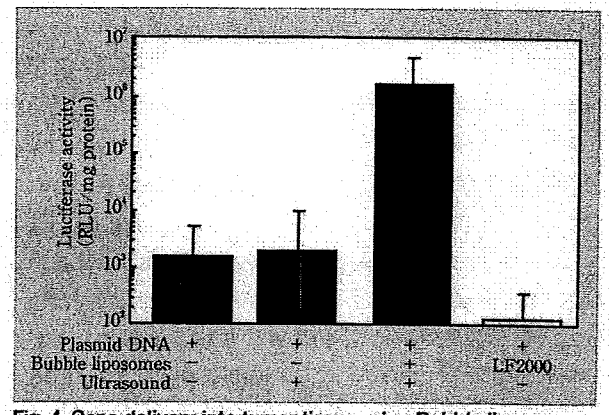

Fig. 4 Gene delivery into tumor tissue using Bubble liposomes and ultrasound

S-180 cells(1×10^6 cells) were inoculated into left foo-tpad of ddY mice. After 4 days, the mice were anaesthetized, then injected with 100μL of pCMV-Luc(10μg) in absent or present of Bubble liposomes(100μg) in PBS. Ultrasound (frequency : 0.7 MHz, duty: 50%; intensity : 1.2W/cm^2, time : 1 minute) was transdermally exposed to tumor tissue. In another experiment, pCMV-Luc(10μg)-Lipofectamine 2000(25μg) complex was suspended in PBS (100μL) and injected into the left femoral artery. After 2 days, tumor tissue was recovered the mice. Luciferase activity was determined.

では遺伝子導入が困難であった部位への遺伝子導入を可能とする技術として期待される。

そこで，腫瘍支配動脈内にバブルリポソームとプラスミドDNAを投与し，血流を介して腫瘍内にバブルリポソームとプラスミドDNAが供給されたところで，腫瘍組織に向け体外から超音波照射し腫瘍組織への遺伝子導入の可能性を評価した。本検討では，市販の遺伝子導入試薬として汎用されているリポフェクタミン2000を用い遺伝子導入活性について比較検討した。その結果，リポフェクタミン2000による遺伝子導入では遺伝子発現が低レベルであり，遺伝子ががん組織にほとんど導入されていないことが明らかとなった。

一方，バブルリポソームと超音波照射の併用群では，がん組織での高い遺伝子発現が認められた(**Fig. 4**)。このように，バブルリポソームと超音波照射の併用で高い遺伝子導入活性が認められたのは，血流を介してがん組織に流れ込んできたバブルリポソームが超音波照射によるキャビテーションで一気に崩壊し，その時発生するジェット流により瞬時に遺伝子ががん組織に導入されたためであると考えられた。このように，バブルリポソームと超音波の併用は，既存の非ウイルスベクターシステムでは遺伝子導入困難である部位にも遺伝子導入可能な新

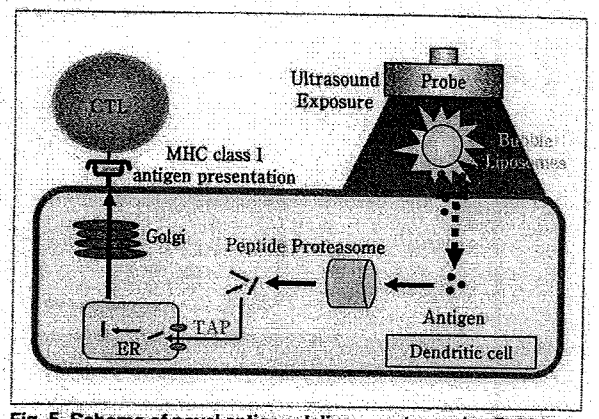

Fig. 5 Schema of novel antigen delivery system using Bubble liposomes and ultrasound

たな遺伝子導入システムとして期待される。

3．バブルリポソームと超音波照射の併用による抗原デリバリー

Boonらのグループによりヒトメラノーマのがん関連抗原が同定されて以来，今日までにさまざまながん関連抗原が同定されている[12]。これに伴い，がんに対する免疫療法が現実的なものとなりつつある。このがん免疫療法を有効な治療法として確立していくためには，がん細胞に対する細胞傷害性T細胞(CTL)を活性化することが重要である。そのためには，T細胞への強力な抗原提示細胞として知られている樹状細胞のMHCクラスⅠ分子上にがん関連抗原を提示させる必要がある。しかし，一般的に外来性抗原はエンドサイトーシス経路で取り込まれ，主にMHCクラスⅡに提示されてしまう。これでは，がん細胞特異的なCTLを活性化できず，有効な抗腫瘍免疫を誘導することは困難である。それゆえ，外来性抗原であっても樹状細胞のMHCクラスⅠに抗原提示させ得る抗原送達システムの開発が必要とされている。

そこでわれわれは，細胞質内に直接外来性物質を導入可能なシステムとしてバブルリポソームと超音波の併用法に着目した。バブルリポソームのキャビテーション誘導時に発生するジェット流を利用して，外来性抗原を樹状細胞の細胞質内に導入することができれば，導入された抗原が樹状細胞のあたかも内在性抗原として認識されMHCクラスⅠに抗原提示誘導されるのではないかと期待される(**Fig. 5**)。そこで，樹状細胞がん免疫療法における新規抗原送達法としてのバブルリポソームと超音波照射の併用法の有用性を評価した。まずはじめに，本方法を用いた際の樹状細胞の細胞質内への抗原送達につい

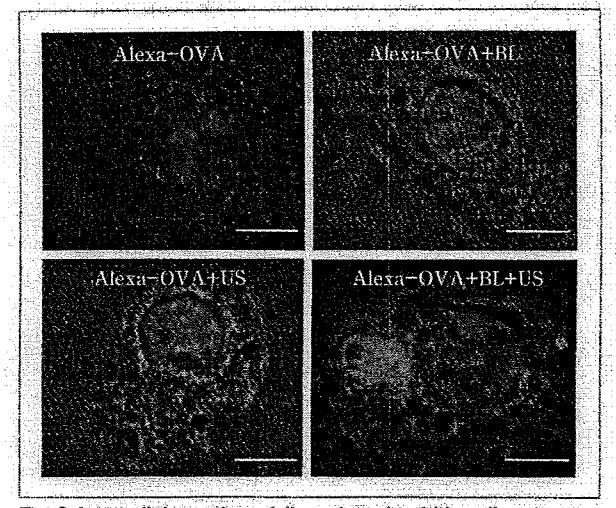

Fig. 6 Intracellular antigen delivery into dendritic cells using Bubble liposomes and ultrasound
Intracellular delivery of Alexa Fluor 488 labeled ovalbumin (Alexa-OVA) into dendritic cells using Bubble liposomes and ultrasound. dendritic cells were pretreated with OptiMEM containing 10mM NaN_3 for 1 h at 4 ℃ to inhibit the endocytosis pathway. After washing the cells, Alexa-OVA was added to the dendritic cells in OptiMEM containing 10mM NaN_3. Then, the dendritic cells were exposed to US in the presence or absence of Bubble liposomes. After ultrasound exposure, the dendritic cells were washed with PBS containing 10mM NaN_3, fixed, and the nuclei were stained with propidium iodide. Intracellular trafficking of Alexa-OVA in the dendritic cells was observed using a confocal laser microscope. Scale bar shows 5 μm. BL : Bubble liposomes, US : ultrasound

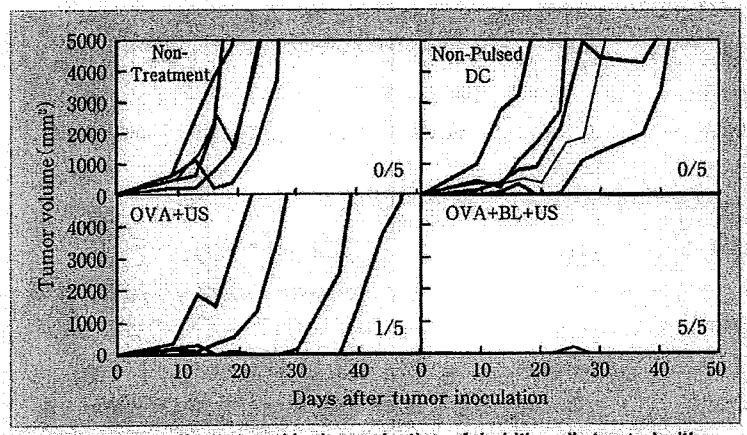

Fig. 7 Antitumor effect caused by immunization of dndritic cells treated with antigen, Bubble liposomes and ultrasound exposure
C57BL/6 mice were immunized with dendritic cells twice. Seven days after the second immunization, E.G7-OVA cells were intradermally inoculated into the backs of the mice, and the tumor volume and survival of the mice was monitored. Tumor volume of the mice after tumor inoculation. Each line indicates the tumor volume in an individual mouse. The fractional number in the lower right of each group shows the number of mice completely rejecting tumors/the number of total experimental mice. OVA : ovalbumin, BL : Bubble liposomes, US : ultrasound

て検討した。その結果，樹状細胞のエンドサイトーシスを阻害した条件下でもバブルリポソームと超音波の併用群では，抗原を細胞質内に導入可能であることが明らかとなった（Fig. 6）。そこで，本方法で抗原送達した樹状細胞をマウスに免疫したときの抗腫瘍効果を検討したところ，がん細胞の完全拒絶が認められた（Fig. 7）。これは，バブルリポソームと超音波の併用により抗原送達した樹状細胞を免疫することで，がん細胞特異的な抗腫瘍免疫が活性化されたためであると考えられた。なお，データには示していないが，抗原特異的なCTLが誘導されていることを確認している。このように，バブルリポソームと超音波照射の併用による抗原送達法は，樹状細胞がん免疫療法における有望な新規抗原送達法になるものと期待される。

まとめ

本稿では，バブルリポソームの超音波造影剤としての可能性や遺伝子導入に関する研究を紹介した。特にバブルリポソームと超音波の併用による遺伝子導入は，短時間の超音波照射で細胞内に遺伝子導入可能であるうえ，既存の非ウイルスベクターシステムより効率のよい遺伝子導入を可能とする有望な遺伝子導入法として期待される。今回はデータに示していないが，われわれはバブルリポソームとプラスミドDNAをマウスの尾静脈から全身投与し，体外から心臓や肝臓に向けて超音波照射することで超音波照射組織特異的に遺伝子導入可能であることも見出している。このように，本方法は，遺伝子治療分野で課題となっている部位特異的な遺伝子発現用ベクター開発において有望な技術であると考えられる。また，樹状細胞への抗原送達に超音波を利用する試みは，これまでに類を見ない新規性の高い方法であり，がん免疫療法における新規抗原送達方法として今後の発展を期待したい。

さて，冒頭でも述べたようにバブルリポソームはリポソーム技術を基盤としたバブル製剤であり，リポソーム表面に容易に標的指向性分子を修飾することができる。今回紹介しなかったが，これまでに著者らの共同研究者はバブルリポソーム表面に血栓を認識するペプチドを修飾し，血栓モデル動物に静脈内投与することで，バブルリポ

ソームの血栓部位への集積を超音波造影により確認している。さらに，この集積したバブルリポソームにキャビテーションを誘導するような周波数・強度の超音波を体外から照射することで血栓を破壊し血流を再開することが可能であることも確認している。このように，バブルリポソームと超音波の併用は，単に細胞にさまざまな物質を導入するだけでなく，これまで超音波造影では診断できなかった血栓の診断を可能にし，さらに治療用超音波照射により血栓治療も行えるような次世代型医療システムの構築を予感させる。それゆえ，今回紹介したような特性を有するバブルリポソームが，次世代型バブル製剤として超音波診断のみならず超音波治療・超音波遺伝子導入ツールに利用され，新たな医療システム構築に貢献できることを期待したい。

謝辞

本稿で紹介した研究は，帝京大学 薬学部 生物薬剤学教室で行われた研究であり，研究遂行にご協力いただいた学生諸子に深謝する。

■引用文献

1) H. Yanagie, K. Maruyama, T. Takizawa, O. Ishida, K. Ogura, T. Matsumoto, Y. Sakurai, T. Kobayashi, A. Shinohara, J. Rant, J. Skvarc, R. Ilic, G. Kuhne, M. Chiba, Y. Furuya, H. Sugiyama, T. Hisa, K. Ono, H. Kobayashi and M. Eriguchi : Journal 60, 43-50(2006)
2) Y. Miyajima, H. Nakamura, Y. Kuwata, J. D. Lee, S. Masunaga, K. Ono and K. Maruyama : Journal 17, 1314-1320(2006)
3) M. Harata, Y. Soda, K. Tani, J. Ooi, T. Takizawa, M. Chen, Y. Bai, K. Izawa, S. Kobayashi, A. Tomonari, F. Nagamura, S. Takahashi, K. Uchimaru, T. Iseki, T. Tsuji, T. A. Takahashi, K. Sugita, S. Nakazawa, A. Tojo, K. Maruyama and S. Asano : Journal 104, 1442-1449(2004)
4) R. Suzuki, T. Takizawa, Y. Kuwata, M. Mutoh, N. Ishiguro, N. Utoguchi, A. Shinohara, M. Eriguchi, H. Yanagie and K. Maruyama : Journal 346, 143-150(2008)
5) O. Ishida, K. Maruyama, H. Tanahashi, M. Iwatsuru, K. Sasaki, M. Eriguchi and H. Yanagie : Journal 18, 1042(2001)
6) R. Suzuki, T. Takizawa, Y. Negishi, N. Utoguchi, K. Sawamura, K. Tanaka, E. Namai, Y. Oda, Y. Matsumura and K. Maruyama : Journal 125, 137-144(2008)
7) R. Suzuki, T. Takizawa, Y. Negishi, K. Hagisawa, K. Tanaka, K. Sawamura, N. Utoguchi, T. Nishioka and K. Maruyama : Journal 117, 130(2007)
8) R. Suzuki, Y. Oda, N. Utoguchi, E. Namai, Y. Taira, N. Okada, N. Kadowaki, T. Kodama, K. Tachibana and K. Maruyama : Journal 133, 198-205(2009)
9) Y. Negishi, Y. Endo, T. Fukuyama, R. Suzuki, T. Takizawa, D. Omata, K. Maruyama and Y. Aramaki : Journal 132, 124-130(2008)
10) T. Yamashita, S. Sonoda, R. Suzuki, N. Arimura, K. Tachibana, K. Maruyama and T. Sakamoto : Journal 85, 741-748(2007)
11) K. Yanagisawa, F. Moriyasu, T. Miyahara, M. Yuki and H. Iijima : Journal 33, 318-325(2007)
12) P. van der Bruggen, C. Traversari, P. Chomez, C. Lurquin, E. De Plaen, B. Van den Eynde, A. Knuth and T. Boon : Journal 254, 1643-1647(1991)

Biochemical and Biophysical Research Communications 388 (2009) 667–671

Contents lists available at ScienceDirect

Biochemical and Biophysical Research Communications

journal homepage: www.elsevier.com/locate/ybbrc

Novel protein engineering strategy for creating highly receptor-selective mutant TNFs

Tetsuya Nomura [a,b,1], Yasuhiro Abe [a,1], Haruhiko Kamada [a,c], Masaki Inoue [a], Tomoyuki Kawara [a,b], Shuhei Arita [a,b], Takeshi Furuya [a,b], Yasuo Yoshioka [b,c], Hiroko Shibata [a], Hiroyuki Kayamuro [a,b], Takuya Yamashita [a,b], Kazuya Nagano [a], Tomoaki Yoshikawa [a,b], Yohei Mukai [b], Shinsaku Nakagawa [b,c], Madoka Taniai [d], Tsunetaka Ohta [d], Shin-ichi Tsunoda [a,b,c,*], Yasuo Tsutsumi [a,b,c]

[a] National Institute of Biomedical Innovation (NiBio), 7-6-8 Saito-Asagi, Ibaraki, Osaka 567-0085, Japan
[b] Graduate School of Pharmaceutical Sciences, Osaka University, 1-6 Yamadaoka, Suita, Osaka 565-0871, Japan
[c] The Center for Advanced Medical Engineering and Informatics, Osaka University, 1-6 Yamadaoka, Suita, Osaka 565-0871, Japan
[d] Hayashibara Biochemical Laboratories Inc., 675-1 Fujisaki, Okayama 702-8006, Japan

ARTICLE INFO

Article history:
Received 4 August 2009
Available online 13 August 2009

Keywords:
Tumor necrosis factor (TNF)
Gene shuffling
Phage display technique
Protein engineering
TNF receptor-selective mutant

ABSTRACT

Tumor necrosis factor (TNF) plays important roles in host defense and in preventing tumor formation by acting via its receptors, TNFR1 and TNFR2, functions of which are less understood. To this end, we have been isolating TNF receptor-selective mutants using phage display technique. However, generation of a phage library with large repertoire (>10^8) is impeded by the limited transformation efficiency of *Escherichia coli*. Therefore, it is currently difficult to create a mutant library containing amino acid substitutions in more than seven residues. To overcome this problem, here we have used two different TNF mutant libraries, each containing random substitutions at six selected amino acid residues, and utilized a gene shuffling method to construct a randomized mutant library containing substitutions at 12 different amino acid residues of TNF. Consequently, using this library, we identified TNF mutants with greater receptor-selectivity and enhanced receptor-specific bioactivity than the existing mutants.

Introduction

Tumor necrosis factor-α (TNF) plays a critical role in host defense through regulation of cell survival, death, and inflammation by acting via one of its receptors, TNFR1 and TNFR2 [1]. Because excess or uncontrolled activity of TNF is often a cause for many immunological diseases and tumor development [2,3], biological drugs such as recombinant TNFs (for enhancement of TNF signaling) or anti-TNF monoclonal antibodies (Mab) and soluble TNF receptors (for neutralization of TNF signaling) have made significant impacts in the treatment of inflammatory diseases and in tumor therapy [4,5]. A number of published reports, however, suggested that neutralization of TNF resulted in increased risk of bacterial infection and several other side effects because of the blocking of signaling via both TNFR1 and TNFR2 [4,5]. Therefore, there is an urgent need to fully understand the biology of the TNF receptor mediated signaling pathway and to develop novel drugs for therapeutic use in TNF-related immunological diseases. For this purpose, TNF receptor-knockout mice were used to understand the relationship between the function of the TNF receptors and TNF-related diseases [8–10]. Recently, it was revealed that the two receptors worked together by crosstalk signaling, which suggested that the TNF-mediated signaling in the presence of both TNF receptors actually correlates with their physiological functions [1,6,7]. To elucidate the roles of TNFR1 and TNFR2, many researchers used an agonistic or an antagonistic TNF mutant that selectively binds to one of the receptors and initiates the biological activity of that specific receptor. These mutant TNFs might be a promising new class of TNF-related drugs without any side effect, and could as well serve as a tool for analyzing the receptor function. Development of these mutant TNFs has facilitated understanding of the molecular interaction between the TNF and its receptors, TNFR1 and TNFR2. In this context, it is noteworthy that several approaches have been undertaken to establish quantitative correlation between the receptor subtype specific-biological activity and the structural and kinetic binding parameters of a receptor-specific TNF mutant [8]. Mutational analysis of single amino acid residues revealed that amino acids at positions 15, 31–35, 84–87, 117, 119 and 143–148, which are clustered throughout in hotspots, greatly contributed to the biological activity of TNF [9,10].

* Corresponding author. Address: Laboratory of Pharmaceutical Proteomics, National Institute of Biomedical Innovation, 7-6-8 Saito-Asagi, Ibaraki, Osaka 567-0085, Japan. Fax: +81 72 641 9817.
E-mail address: tsunoda@nibio.go.jp (S.-i. Tsunoda).
[1] These authors contributed equally to the work.

0006-291X/$ - see front matter © 2009 Elsevier Inc. All rights reserved.
doi:10.1016/j.bbrc.2009.08.052

With a similar goal in mind, we previously constructed M13 bacteriophage libraries (Library I and Library II) displaying mutant TNFs randomized at amino acid positions 29, 31, 32, 145, 146 and 147 or at positions 84–89 of TNF, and succeeded in isolating agonistic- and antagonistic-mutant TNFs from these libraries [11,12]. Particularly, the TNFR1-selective antagonist mutTNF-T2 showed almost same therapeutic effect as the anti-TNF biologics in a hepatitis model [13].

Currently, generation of a phage-displayed library with large repertoire (>10^8) is impeded by the limited transformation efficiency of *Escherichia coli* (*E. coli*). As a result, it is difficult to construct a high quality mutant library ($20^6 = 6.4 \times 10^7$) that is randomized at more than seven different amino acid residues and includes almost all clones. To overcome this problem, here we have developed a novel protein engineering strategy (gene shuffling method) for creation of functional mutant proteins. To achieve our goal, we first constructed two types of phage libraries displaying mutant TNFs, in each of which six amino acids residues in the predicted receptor binding sites were replaced with other amino acid residues, and these phage display libraries were subsequently subjected to several rounds of panning against TNFR1 and TNFR2, respectively, using a surface plasmon resonance analyzer (BIAcore). After several rounds of panning, we obtained two libraries, each one containing enriched number of a TNF receptor-specific high affinity clones. Next, we utilized these enriched libraries to construct high quality TNF receptor-specific shuffling libraries using a gene shuffling method. Finally, panning of these shuffling libraries against TNFR1 and TNFR2, respectively, have allowed us to isolate TNF mutants with greater receptor-selectivity and enhanced receptor-specific bioactivity than the previously isolated TNFR1-selective mutant R1-5 and TNFR2-selective mutant R2-3 [12].

Materials and methods

Cell culture. HEp-2 cells (a human fibroblast cell line) were provided by the Cell Resource Center for Biomedical Research (Tohoku University, Sendai, Japan) and were maintained in RPMI 1640 medium (Sigma-Aldrich Japan, Tokyo, Japan) supplemented with 10% FBS and antibiotics cocktail (penicillin 10,000 units/ml, streptomycin 10 mg/ml, and amphotericin B 25 μg/ml; Nacalai tesque, Kyoto, Japan). hTNFR2/mFas-preadipocyte (mouse preadipocyte cell expressing a chimeric receptor, which consist of the extracellular and transmembrane domain of human TNFR2 and the intracellular domain of mouse Fas) cells were established previously in our laboratory [14] and were maintained in D-MEM (Wako Pure Chemical Industries, Osaka, Japan) supplemented with blasticidin S HCl (5 μg/ml Sigma-Aldrich Japan, Tokyo, Japan), 10% FBS, 1 mM sodium pyruvate, 5×10^{-5} M 2-mercaptoethanol, and antibiotic cocktail.

Selection of TNF receptor-selective mutants from the mutant TNF phage display library by panning. Human TNFR1 Fc chimera or human TNFR2 Fc chimera (R&D systems, Minneapolis, MN) was immobilized onto a CM3 sensor chip (GE Healthcare, Buckinghamshire, UK) as described previously [11,12]. The phage display library (1×10^{11} CFU/100 μl) was injected over the sensor chip at a flow rate of 3 μl/min on BIAcore. After binding, the chip was rinsed until the association phase was reached. Elution was carried out using 4 μl of 10 mM glycine–HCl. The eluted phage pool was neutralized with 1 M Tris–HCl (pH 6.9). Next, the phages in the eluted pool were amplified in the *E. coli* TG1. The panning, elution and amplification steps were repeated twice. Subsequently, single clones were isolated from the phage pool, and the DNA sequences of phagemids purified from the single clones were analyzed.

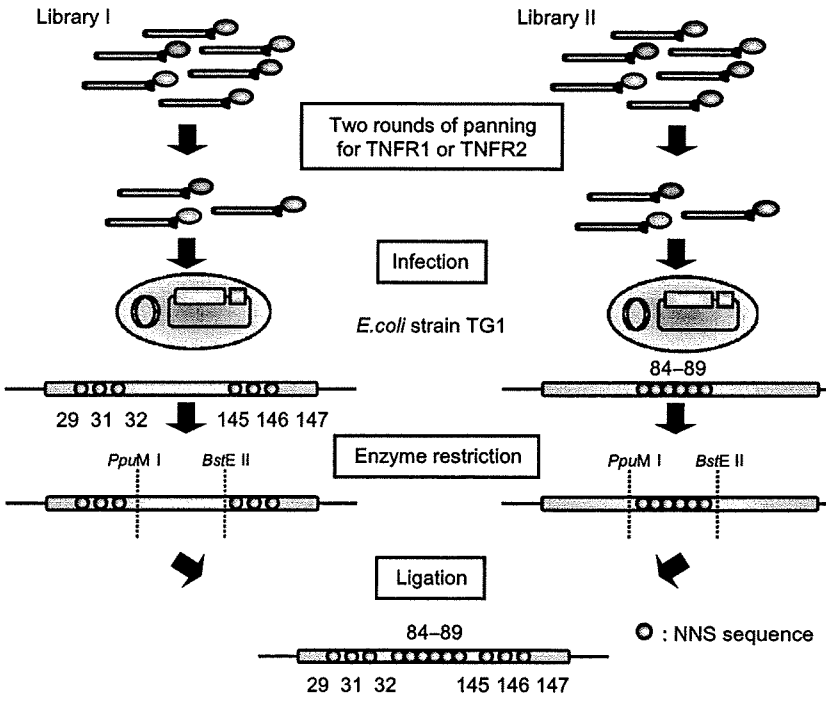

Fig. 1. Construction of the Gene Shuffling Library. Schematic description of the methods used to construct the Gene Shuffling Libraries A and B from two parent mutant TNF libraries, each one of which was created by replacing the codon of the amino acid residue at positions 29, 31, 32, 145, 146 and 147 (Library I) or at positions 84, 85, 86, 87, 88 and 89 (Library II) of TNF with the randomized codon NNS (where N and S represent G/A/T/C or G/C, respectively) to obtain all twenty amino acid substitutions at each position. NNS encodes all 20 different amino acids. Mutations were introduced by PCR using the lysine-deficient mutant TNF as the template as described in Materials and methods.

Construction of mutant TNF phage library (Gene Shuffling Library). The pCANTAB phagemid vector encoding a lysine-deficient mutant TNF which was created previously was used as a template for library construction [15]. First, two types of phage libraries, displaying mutant TNFs containing random substitutions of amino acid residues at positions 29, 31, 32, 145, 146 and 147 (Library I), and at positions 84, 85, 86, 87, 88 and 89 (Library II), were prepared using polymerase chain reaction (PCR) as described earlier [11,12]. Each library was then subjected to two rounds of panning against TNFR1 to concentrate TNFR1-specific high-affinity mutant TNFs. Next, we purified all plasmids from each concentrated libraries. These two pools of purified plasmids were digested with the restrict enzymes (*Ppu*MI, *Bst*EII), DNA inserts were purified and then ligated to a pY03′ phagemid vector to construct a randomized library (Shuffling Library A) that contained mutations at twelve different amino acid residues (see Fig. 1). We also prepared a second randomized library (Shuffling Library B) by following the same protocol and using TNFR2 for panning.

Competitive ELISA. Inhibition of wtTNF binding to the TNFR1 and TNFR2 by a TNFR1 or TNFR2-selective mutant was measured using ELISA as described previously [16]. The wtTNF-FLAG, a FLAG tag fusion protein of human TNF [16], was used as a marker protein. Briefly, the immune assay plates (NUNC, Roskilde, Denmark) were coated with 5 μg/ml goat anti-human IgG antibody (MP Biomedicals, Aurora, OH) and incubated with 0.2 μg/ml of either the human TNFR1 or the human TNFR2. After blocking the non-specific binding sites, a pre-made mixture containing 100 ng/ml of wtTNF-FLAG and various concentrations of a given TNF mutant was added to the wells. After 2 h of incubation at room temperature, the wells were washed. Next, 0.5 μg/ml biotinylated anti-FLAG M2 antibody was added to each well and then the plate was incubated for an additional period of 2 h at room temperature. Wells were washed and then incubated with the horseradish peroxidase-coupled streptavidin (Zymed Lab. Inc., South San Francisco, CA) for 30 min at room temperature. The remaining bound wtTNF-FLAG was quantified as described above.

Assay for cytotoxicity mediated via TNFR1 and TNFR2. To measure cytotoxicity mediated via the TNFR1, HEp-2 cells (4×10^4 cells/well) were cultured in 96-well plates (NUNC, Roskilde, Denmark) in presence of a given TNF mutant, serially diluted human wtTNF (Peprotech, Rocky Hill, NJ), and with 100 μg/ml cycloheximide for 18 h, and cytotoxicity was assessed by using the methylene blue assay as described previously [17]. To measure cytotoxicity mediated via the TNFR2, hTNFR2/mFas-preadipocyte cells (1×10^4 cells/well) were cultured in the 96-well plates (NUNC) in presence of a given TNF mutant and serially diluted human wtTNF for 48 h, and then cell survival was determined by using the methylene blue assay.

Results and discussion

In this study, to overcome the barrier of limited transformation efficiency of *E. coli* in the preparation of high quality phage display libraries, we adopted a novel protein engineering technology in which amino acid residues at 12 different places were randomly substituted using a gene shuffling method to enhance the usefulness of the phage display technique.

Fig. 1 schematically summarizes the protocol used for constructing a novel TNF gene shuffling library. First, we prepared two phage libraries displaying mutant TNFs, in each of which six different amino acid residues (residues at positions 29, 3, 32, 145, 146 and 147 for Library I; residues at positions from 84 to 89 for Library II) present in the receptor binding site of TNF, previously identified by point mutation analysis and X-ray crystallography, were randomly substituted with other amino acid residues [11,12]. The phage libraries expressing mutant TNFs were constructed by two-step PCR as described in the Materials and methods. We confirmed that the phage Libraries I and II consisted of 8×10^6 and 6×10^6 independent clones, respectively (*data not shown*). Next, to enrich for TNFR1 binding mutants, we subjected each library to two rounds of panning using TNFR1 and recovered phage clones with high affinity to TNFR1. We used a gene shuffling method to construct the mutant TNF Shuffling Library A from these libraries, which consist of high affinity clones to TNFR1 (see Fig. 1). In the similar manner, we constructed the Shuffling Library B by carrying out panning using TNFR2. Amino acid analysis of eight randomly picked clones from each library revealed that each one of them was a mutant containing amino acid substitutions at 12 residues (*results not shown*). To concentrate TNFR1-selective mutant TNFs, the Shuffling Library A was subjected to two rounds of panning against TNFR1 using the BIAcore biosensor. After the second panning, supernatants of *E. coli* TG1 included phagemid were randomly collected and performed the screening by ELISA and bioassay to analyze their bioactivity and affinity against TNFR1 (*data not shown*). As a result, we identified six TNFR1-selective, high affinity clones, R1-15 to R1-20 (Table 1). Similarly, we identified three TNFR2-selective candidates (R2-14 to R2-16) from the Shuffling Library B (Table 1). The fact that the amino acid residue at position 87 in all active TNF receptor-selective candidates was a Tyr residue (Table 1), it suggests that Tyr87 is an important residues

Table 1
Substituted residues and affinities of TNF receptor-selective mutant candidates.

	Amino acid sequence												Relative affinity (%)[a]		
	29	31	32	84	85	86	87	88	89	145	146	147	TNFR1	TNFR2	TNFR1/TNFR2
wtTNF	L	R	R	A	V	S	Y	Q	T	A	E	S	100.0	100.0	1.0
R1-5[b]	K	A	G	–	–	–	–	–	–	–	S	T	82.0	2.0×10^{-2}	4.1×10^3
R1-15	R	N	Y	S	–	R	–	N	P	–	–	–	115.7	6.0×10^{-2}	1.9×10^3
R1-16	T	Q	Y	T	P	G	–	S	H	–	A	H	8.6	6.0×10^{-2}	1.4×10^2
R1-17	R	T	F	S	P	L	–	R	Q	S	S	T	54.2	6.0×10^{-2}	9.0×10^2
R1-18	K	N	F	S	S	H	–	T	H	–	–	–	53.9	1.0×10^{-1}	5.4×10^2
R1-19	S	N	Y	–	–	–	–	–	–	–	V	–	138.7	8.0×10^{-1}	1.7×10^3
R1-20	T	–	Y	S	H	T	–	P	S	S	Q	A	170.5	3.0×10^{-2}	5.7×10^3
R2-3[c]	–	–	–	–	–	–	–	–	–	R	–	T	<0.1	33.4	<0.0029
R2-14	–	–	–	–	P	–	–	N	S	S	A	D	1.6	103.7	0.0154
R2-15	–	–	–	S	Q	A	–	N	–	I	G	D	<0.1	141.8	<0.0007
R2-16	–	–	–	–	–	–	–	–	–	H	S	D	1.4	91.7	0.0152

Comparison of the amino acid residues of the wild-type and mutant TNFs; conserved residues are indicated using a dash.
[a] Concentration of mutant TNF required for 50% inhibition of maximal binding of wtTNF-FLAG.
[b] A TNFR1-selective mutant, which was isolated previously from the existing phage library (Library I).
[c] A TNFR2-selective mutant, which was isolated obtained from the existing phage library (Library I).

for receptor binding, which is in good agreement with the previous report [8–10].

To determine the properties of the receptor-selective candidates, we purified all the candidate TNF mutants as recombinant proteins using a general recombinant protein technology [11,12,15,18]. After each recombinant mutant TNF was expressed in *E. coli* BL21λDE3 and purified to homogeneity, we used gel electrophoresis and gel filtration chromatography to confirm that each of them, like the wtTNF, displayed MW of 17 kDa and formed a homotrimeric complex (*results not shown*). We next used a competitive ELISA to examine the binding properties of the mutant TNFs to the TNF receptors, and the results are summarized in Table 1. As summarized, all TNFR1-selective candidates showed lower affinity for TNFR2 than the wtTNF. On the other hand, affinities of the clones R1-15, R1-19, and R1-20 for TNFR1 were better than that the wtTNF. Especially, affinity of the clone R1-20 for TNFR1 was more than 1.7-fold higher than that of the wtTNF and was about 2-fold higher than that of the TNF mutant R1-5, which was previously identified from the Library I [12]. Additionally, selectivity of R1-20 for TNFR1 was higher than that of the R1-5. Next, we evaluated affinity of the TNFR2-selective mutants for TNFR2 (Table 1). Our results revealed that the clones R2-14, R2-15 and R2-16 bound to TNFR2 more strongly than the TNF mutant R2-3, which was previously isolated in our laboratory [12]. Especially, the TNF mutant R2-15 bound to TNFR2 with an affinity that was 1.4-fold higher than that of the wtTNF. R2-15 also showed superior TNFR2-selectivity than R2-3. Thus, by using the gene shuffling libraries, we were able to isolate TNF mutants that were highly receptor-selective. The receptor-selective TNF mutants R1-20 and R2-15 contained amino acid substitutions at 10 and 7 places, respectively. A point mutation analysis study of TNF suggested that the amino acid residues near position 140 are essential for TNFR1 binding [8,10,12]. In agreement with this report, we found that the residue at position 145 in the TNFR1-specific mutants is mostly retained or contained conservative amino acid substitutions, whereas more than one residues at positions 145, 146 and 147 in the TNFR2-selective mutants contained non-conservative amino acid substitutions. On the other hand, the amino acids residues near positions 30 and 80 were mostly conserved in the TNFR2-specific mutants, but not in the TNFR1-specifc mutants, suggesting that these amino acid residues might play important roles in TNFR2 binding [12]. Thus, this is the first report describing the creation of highly receptor-selective TNF mutants, namely R1-20 and R2-15, from a randomized mutant TNF library containing amino acid substitutions at 12 different amino acid residues. These results clearly demonstrate the usefulness of the developed method, which combines both phage display and gene shuffling techniques.

Next, we examined the receptor-selective bioactivities of the TNF mutants R1-20 and R2-15, each one of which showed highest receptor-selectivity, and the results are shown in Fig. 2 and Table 2. TNFR1-mediated cytotoxicity induced by the TNF mutant R1-20, as measured *in vitro* using the Hep-2 cells, was 7-fold and 2.2-fold higher than those of the mutant R1-5 and wtTNF, respectively (Fig. 2A and Table 2). Next, we evaluated the TNFR2-mediated activity of R1-20 using the hTNFR2/mFas-preadipocyte cells, which were previously constructed in our laboratory [14]. As expected, R1-20 hardly exhibited bioactivity via TNFR2, and the activity was much lower than that of the wtTNF (Fig. 2B and Table 2). On the other hand, the bioactivity of the TNFR2-selective mutant R2-15 via TNFR1 was 1000-fold lower than that of the wtTNF (Fig. 2C). The bioactivity of R2-15 via TNFR2 was, however, 2.5-fold higher than that of the wtTNF and more than 15-fold higher than that of the R2-3 mutant (Fig. 2D and Table 2). Remarkably, the bioactivity of R2-15 was higher that that of the R2-3, both of which are TNFR2-specific TNF mutants (Fig. 2D and Table 2).

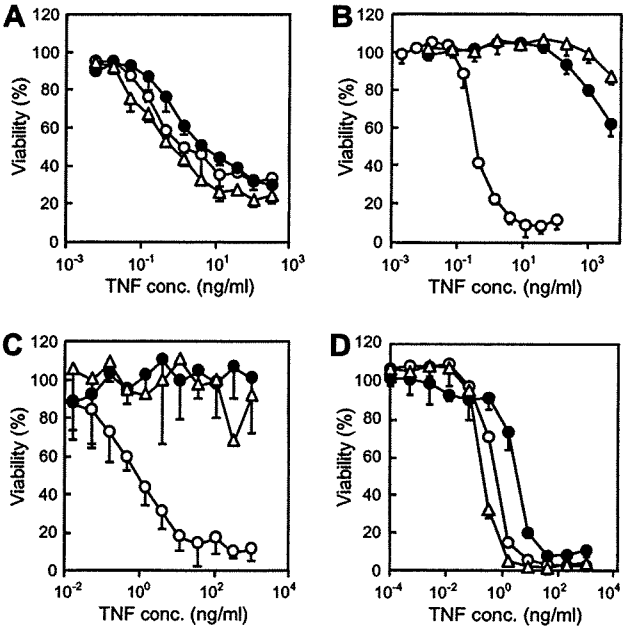

Fig. 2. Bioactivity of the receptor-selective mutants. The receptor-specific bioactivity (% viability) was measured following the treatment of HEp-2 or hTNFR2/mFas-preadipocyte cells with the wild-type or mutant TNF by using the methylene blue staining procedure as described in Materials and methods. (A) and (C) TNFR1-mediated bioactivity was measured using the HEp-2 cells. (B) and (D) TNFR2-mediated bioactivity was measured using the hTNFR2/mFas-preadipocyte cells. In (A) and (B) open circle, wtTNF; closed circle, R1-5; and open triangle, R1-20. In (C) and (D) open circle, wtTNF; closed circle, R2-3; and open triangle, R2-15.

Table 2
Bioactivity of receptor-selective mutants.

	TNFR1[a]		TNFR2[b]	
	EC50 (ng/ml)	Relative (%)	EC50 (ng/ml)	Relative (%)
wtTNF	1.3	100.0	0.4	100.0
R1-5	4.4	29.5	$>5.0 \times 10^5$	$<8.0 \times 10^{-5}$
R1-20	0.6	216.7	$>5.0 \times 10^5$	$<8.0 \times 10^{-5}$
R2-3	$>1.0 \times 10^3$	<0.1	3.1	13.0
R2-15	$>1.0 \times 10^3$	<0.1	0.2	200.0

The bioactivity values were determined from the results shown in Fig. 2 and are shown here as relative values (% wtTNF). Each value shown is mean ± SD ($n = 3$).

[a] TNFR1-mediated bioactivity was determined by a cytotoxicity assay as described in Materials and methods using the HEp-2 cells.

[b] TNFR2-mediated bioactivity was determined by a cytotoxicity assay as described in Materials and methods using the hTNFR2/mFas-preadipocyte cells.

Thus, by using the combined technology described in this study, we were able to identify TNF mutants with improved TNF receptor-selectivity and enhanced bioactivity than the existing TNF mutants.

Presently, both the underlying mechanism of signal transduction via each TNF receptor, and the relationship between the TNF receptors and onset of TNF-related diseases remain unclear. We anticipate that the TNF receptor-selective TNF mutants found in this study could be used as tools to analyze the receptor-specific signal transduction pathways. Additionally, we believe that the technology described here would be easily applicable to many disease-related proteins of unknown function. Thus, by creating structurally diverse protein libraries, we could rapidly identify therapeutically valuable proteins, which might lead to the development of effective and safe drugs in the near future.